

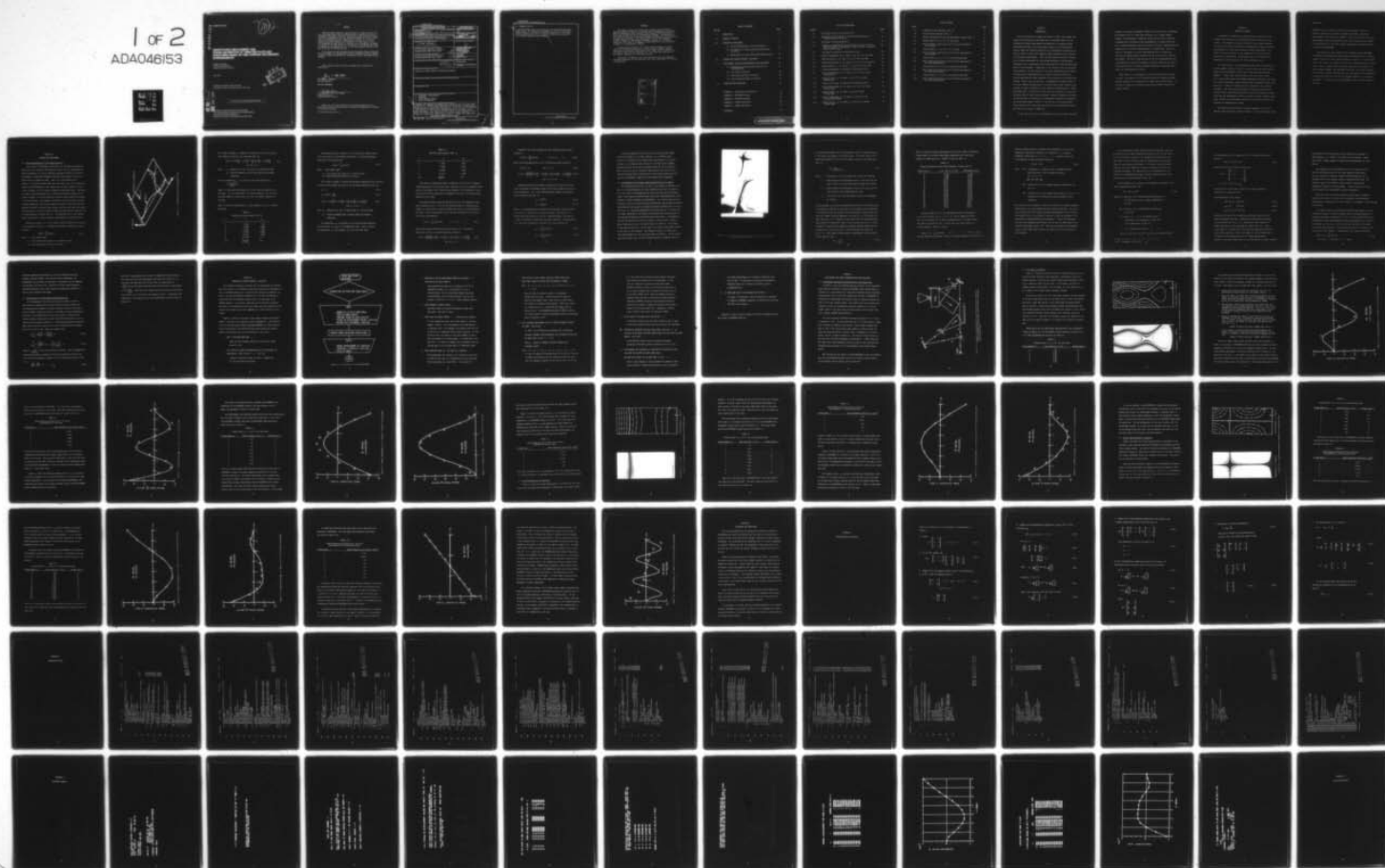
AD-A046 153

AIR FORCE AERO PROPULSION LAB WRIGHT-PATTERSON AFB OHIO F/G 20/11
QUANTITATIVE DISPLACEMENT AND STRAIN DISTRIBUTION OF VIBRATING --ETC(U)
JUL 77 J C MACBAIN
AFAPL-TR-77-44

UNCLASSIFIED

NL

1 of 2
ADA046153



AD A 046153

AFAPL-TR-77-44

104

**QUANTITATIVE DISPLACEMENT AND
STRAIN DISTRIBUTION OF VIBRATING PLATE-LIKE
STRUCTURES BASED ON TIME AVERAGE HOLOGRAPHIC
INTERFEROMETRY**

JAMES C. MacBAIN
PROPULSION BRANCH
TURBINE ENGINE DIVISION

JULY 1977

TECHNICAL REPORT AFAPL-TR-77-44
Final Report for Period 1 October 1976 to 1 June 1977

DDC
RECEIVED
NOV 1 1977
F

Approved for public release; distribution unlimited.

AD No. _____
DDC FILE COPY

AIR FORCE AERO PROPULSION LABORATORY
AIR FORCE WRIGHT AERONAUTICAL LABORATORIES
AIR FORCE SYSTEMS COMMAND
WRIGHT-PATTERSON AIR FORCE BASE, OHIO 45433

NOTICE

When Government drawings, specifications, or other data are used for any purpose other than in connection with a definitely related Government procurement operation, the United States Government thereby incurs no responsibility nor any obligation whatsoever; and the fact that the Government may have formulated, furnished, or in any way supplied the said drawings, specifications, or other data, is not to be regarded by implication or otherwise as in any manner licensing the holder or any other person or corporation, or conveying any rights or permission to manufacture, use, or sell any patented invention that may in any way be related thereto.

This report has been reviewed by the Information Office (ASD/OIP), and is releasable to the National Technical Information Service (NTIS). At NTIS, it will be available to the general public, including foreign nations.

This technical report has been reviewed and is approved for publication.

James C. MacBain

DR. JAMES C. MACBAIN
Project Engineer

FOR THE COMMANDER

I. J. Gershon

I. J. GERSHON, Tech Area Manager
Propulsion Branch
Turbine Engine Division

Copies of this report should not be returned unless return is required by security considerations, contractual obligations, or notice on a specific document.

UNCLASSIFIED

SECURITY CLASSIFICATION OF THIS PAGE (When Data Entered)

REPORT DOCUMENTATION PAGE		READ INSTRUCTIONS BEFORE COMPLETING FORM
1. REPORT NUMBER (14) AFAPL-TR-77-44	2. GOVT ACCESSION NO.	3. RECIPIENT'S CATALOG NUMBER (9)
4. TITLE (and Subtitle) Quantitative Displacement and Strain Distribution of Vibrating Plate-like Structures Based on Time Average Holographic Interferometry.		5. TYPE OF REPORT & PERIOD COVERED Final Report. 1 Oct 1976 - 1 Jun 1977
7. AUTHOR(s) (10) James C. MacBain		6. PERFORMING ORG. REPORT NUMBER
9. PERFORMING ORGANIZATION NAME AND ADDRESS Air Force Aero Propulsion Laboratory Wright-Patterson AFB, Ohio 45433		8. CONTRACT OR GRANT NUMBER(s) (17)
11. CONTROLLING OFFICE NAME AND ADDRESS Air Force Aero Propulsion Laboratory Wright-Patterson AFB, Ohio 45433		10. PROGRAM ELEMENT, PROJECT, TASK AREA & WORK UNIT NUMBERS (16) 646100 3066 12 21 61102F 2307 S2 01
14. MONITORING AGENCY NAME & ADDRESS (if different from Controlling Office) (12) 102P.		12. REPORT DATE (11) July 1977
		13. NUMBER OF PAGES 94
		15. SECURITY CLASS. (of this report) Unclassified
		15a. DECLASSIFICATION/DOWNGRADING SCHEDULE
16. DISTRIBUTION STATEMENT (of this Report) Approved for Public Release, Distribution Unlimited		
17. DISTRIBUTION STATEMENT (of the abstract entered in Block 20, if different from Report) 62203F		
18. SUPPLEMENTARY NOTES		
19. KEY WORDS (Continue on reverse side if necessary and identify by block number) 1. Holographic Interferometry 2. Vibration 3. Finite Element Analysis 4. Strain Determination		
20. ABSTRACT (Continue on reverse side if necessary and identify by block number) A technique for computing the bending strain resulting from the resonant modal deformation of a vibrating plate-like structure is described. Interferometric fringes obtained by time-average holography are used as the basis for generating a mathematically continuous series approximation of the structure's out-of-plane displacement. The terms of the series consist of the eigenfunctions of a simple beam having either clamped-free or free-free boundary conditions. Use is made of a linear least squares equation solver to compute the coefficients (CONTINUED ON REVERSE SIDE OF PAGE)		

DD FORM 1473
1 JAN 73

EDITION OF 1 NOV 65 IS OBSOLETE

UNCLASSIFIED

SECURITY CLASSIFICATION OF THIS PAGE (When Data Entered)

011 570

next page
mt

UNCLASSIFIED

SECURITY CLASSIFICATION OF THIS PAGE(When Data Entered)

20. ABSTRACT (Cont'd)

of the displacement series terms based upon the experimental holographic fringe values. The technique is programmed for use on an interactive computer terminal. The method is tested by comparing it to the results of an eigenvalue analysis of a cantilevered plate analyzed using the finite element computer program, NASTRAN.

UNCLASSIFIED

SECURITY CLASSIFICATION OF THIS PAGE(When Data Entered)

FOREWORD

This report covers work carried out at AFAPL's Turbo Structures Research Laboratory (TSRL) on the quantitative determination of displacements and bending strains resulting from resonant modal deformation of plate-like structures such as turbomachinery blading. The objective of the research effort was to develop a workable technique for efficiently obtaining surface bending strain information from the interferometric fringes produced by time average holographic testing of a vibrating structure. This type of information relates directly to the structural integrity of turbomachinery blading.

The work was performed in the Turbine Engine Division of the Air Force Aero Propulsion Laboratory, Air Force Systems Command, Wright-Patterson Air Force Base, Ohio, under Project 3066, Task 12, Work Unit 21 and Project 2307, Task S2, Work Unit 01. The effort was conducted by Dr. James C. MacBain of the Propulsion Branch.

The author is indebted to Mr. Bruce Tavner for his very competent technical assistance in the laboratory and to Miss Helen Davis for typing the manuscript.

ACCESSION for	
NTIS	Wave Section <input checked="" type="checkbox"/>
DOC	B if Section <input type="checkbox"/>
UNANNOUNCED	<input type="checkbox"/>
JUSTIFICATION	
BY	
DISTRIBUTION/AVAILABILITY CODES	
Di	IL
A	

TABLE OF CONTENTS

SECTION	PAGE
I. INTRODUCTION	1
II. SUMMARY OF RESULTS	3
III. THEORETICAL DEVELOPMENT	5
3.1 Series Approximation of Plate Deformation	5
3.2 Determination of Modal Weighting Coefficients, A_i and B_i	11
3.3 Ramifications of Using Simple Beam Eigenfunctions	19
IV. INTERACTIVE COMPUTER PROGRAM - HOLOCURVE	21
V. DISPLACEMENT AND STRAIN DETERMINATION USING HOLOCURVE	27
5.1 Displacement and Strain Distribution of a Vibrating Plate	27
5.2 Lyre Mode of Vibration	29
5.3 Second Bending Mode of Vibration	38
5.4 Second Torsional Mode of Vibration	44
VI. DISCUSSION AND CONCLUSION	54
APPENDIX A - Pseudoinverse Calculation	55
APPENDIX B - HOLOCURVE Listing	61
APPENDIX C - HOLOCURVE Example	75
APPENDIX D - LLSQAR Description	88
APPENDIX E - INTERP Description	92
REFERENCES	94

LIST OF ILLUSTRATIONS

FIGURE		PAGE
3.1	Coordinate System for Cantilever Plate	6
3.2	Holographic Interferogram of Turbine Blade Vibrating in a Torsional Mode at 25,943 Hz.	12
4.1	Flow Chart for Program Holocurve	22
5.1	Schematic of Experimental Set-up; BS-beam splitter, M-mirror, BE-beam expander, P-photographic plate, S-siren, R-reference beam, O-object beam	28
5.2	Lyre Mode of Vibration for Cantilever Plate	30
5.3	Normal Displacement, W , vs. Span, x , at $y=.5"$ for Lyre Mode	32
5.4	Bending Strain ϵ_x , vs. Span, x , at $y=.5"$ for Lyre Mode	34
5.5	Normal Displacement, W , vs. Chord, y , at $x=2.5"$ for Lyre Mode	36
5.6	Bending Strain, ϵ_y , vs. Chord, y , at $x=2.5"$ for Lyre Mode	37
5.7	Second Bending Mode of Vibration for Cantilever Plate	39
5.8	Normal Displacement, W , vs. Span, x , at $y=.5"$ for Second Bending Mode	42
5.9	Bending Strain, ϵ_x , vs. Span, x , at $y=.5"$ for Second Bending Mode	43
5.10	Second Torsion Mode of Vibration for Cantilever Plate	45
5.11	Normal Displacement, W , vs. Span, x , at $y=.5"$ for Second Torsion Mode	48
5.12	Bending Strain, ϵ_x , vs. Span, x , at $y=.5"$ Second Torsion Mode	49
5.13	Normal Displacement, W , vs. Chord, y , at $x=1.0"$, for Second Torsion Mode	51
5.14	Bending Strain, ϵ_y , vs. Chord, y , at $x=1.0"$ for Second Torsion Mode	53

LIST OF TABLES

TABLE		PAGE
3.1	Clamped-Free Beam Constants (Ref. 6)	7
3.2	Free-Free Beam Constants (Ref. 6)	9
3.3	Normal Displacement Values from Holographic Fringes (Ref. 8)	14
5.1	Fringe Values vs. x , $y=.5"$, for Lyre Mode	29
5.2	Modal Weighting Coefficients for CF Series Approximation of Lyre Mode	33
5.3	Fringe Values vs. y , $x=2.5"$, for Lyre Mode	35
5.4	Modal Weighting Coefficients for FF Series Approximation of Lyre Mode	38
5.5	Fringe Values vs. x , $y=.5"$, for Second Bending Mode	40
5.6	Modal Weighting Coefficients for CF Series Approximation of Second Bending Mode	41
5.7	Fringe Values vs. x , $y=.5"$, for Second Torsion Mode	46
5.8	Modal Weighting Coefficients for CF Series Approximation of Second Torsion Mode	46
5.9	Fringe Values vs. y , $x=1.0"$, for Second Torsion Mode	47
5.10	Modal Weighting Coefficients for FF Series Approximation of Second Torsion Mode	50

SECTION I

INTRODUCTION

Since its discovery by Powell and Stetson in 1965, time average holographic interferometry has developed into an extremely useful tool for studying the resonant mode shapes and frequencies of vibrating bodies. The method has proven to be particularly useful in the turbine engine industry where the vibration properties of turbomachinery blading must be known in order to insure that dangerous blade resonances do not coincide with operating engine speeds. While the mode shape and natural frequency can be directly determined by time average holographic interferometry, knowledge of the corresponding strain distribution for each vibration mode shape is also desirable. Computation of the surface strain has presented some problems in the past because of the error magnification that results in using inexact experimental data to compute the second derivative. Various approaches have been proposed in the literature for attacking this problem. Waters, Aas, and Erf (Ref. 1) determined the bending strain of the first bending vibration mode of a turbine blade using a "smooth curve" approach in order to smooth out errors caused by differentiation. Taylor and Brandt (Ref. 2) carried out a very good error analysis of strain computations based on cubic spline functions. Recently, Dandliker, Ineichen, and Mastner (Ref. 3) reported on an experimental technique for measuring the interference phase to within $.3^\circ$ at any point on the displacement fringe pattern; thus, improving the accuracy of the holographic displacement data by two orders of magnitude.

In the vein of the first two references cited, the present study uses

standard time average holographic fringes as the raw data for determining the bending strain of a plate-like structure, e.g., turbine engine blading. The holographic fringes are used as the raw data to generate a mathematically continuous series approximation of a plate-like structure's normal displacement where the terms of the series approximation are clamped-free or free-free eigenfunctions of a simple beam. Since the series is continuous, it can be differentiated twice to obtain the curvature or bending strain resulting from one of the plate's vibration mode shapes. The use of beam functions in the series approximation has the advantage that the plate's geometric boundary conditions are identically satisfied and its natural boundary conditions, satisfying equilibrium, are approximately satisfied.

What follows is a development of the theory upon which the method is based, a description of the resulting interactive computer program, and some examples of its application to some plate vibration modes. The results are compared with bending strain values obtained using finite element analysis.

SECTION II

SUMMARY OF RESULTS

A technique for computing the bending strain resulting from the resonant modal deformation of vibrating plate-like structures is described. Interferometric fringes obtained by time average holography are used as the basis for generating a mathematically continuous series approximation of a plate-like structure's normal displacement. The terms of the series consist of the clamped-free or free-free eigenfunctions of a simple beam. The bending strain is then obtained by computing the second derivative of the displacement series.

The coefficients of the displacement series terms are computed for a given segment (length or width) of a cantilevered plate-like structure based upon the holographic fringe values lying along the same plate segment. A linear least squares solution routine is used to solve for p series coefficients, called modal weighting coefficients, in terms of k normal displacement values obtained from k holographic fringe values where $k \geq p$. A "best fit" solution is thus obtained for the plate displacement. This least squares approach in conjunction with the fact the beam series functions exactly satisfy the plate's geometric boundary conditions and approximately satisfy the plate's natural boundary conditions, results in a displacement series that yields quite accurate displacement and bending strain values.

The technique described above has been programmed for use on a Tektronix 4010 interactive computer terminal. To use the program, called

HOLOCURVE, the user specifies the particular chordwise (free-free boundary conditions) or spanwise (clamped-free boundary conditions) plate segment to be studied, the number of terms to be used in the series approximation, and the holographic fringe values along the plate segment. A listing and plot of the plate's normal displacement and bending strain is generated by HOLOCURVE.

The accuracy and effectiveness of the technique used by HOLOCURVE is checked by determining the displacement and bending strain at selected segment locations for three different modes of vibration of a cantilevered plate. The results are compared to those of an eigenvalue analysis carried out on a finite element model of the plate using the finite element computer program, NASTRAN. The HOLOCURVE results are in excellent agreement with the finite element analysis except for cases where the bending strain is essentially zero as in the case of chordwise segment for a torsional mode shape. In cases such as this, HOLOCURVE issues a warning message to the user.

SECTION III

THEORETICAL DEVELOPMENT

3.1 Series Approximation of the Plate Deformation

In the spirit of Rayleigh's method (Ref. 4), introduced one hundred years ago in his treatise, "The Theory of Sound", one can approximate the normal deformation of a freely vibrating rectangular plate by the natural mode shapes of beams whose boundary conditions are similar to those of a plate along its respective edges. Thus, for a cantilevered plate (Figure 3.1), having one edge fixed and three edges free, one can model the plate's modal deformation in the clamped-free direction (parallel to the x axis in Figure 3.1) by a similar clamped-free beam mode shape. Similarly, the plate's modal deformation in its free-free direction (parallel to the y axis in Figure 3.1) can be modeled by suitably chosen natural mode shapes of a free-free beam. The boundary conditions of the plate and the corresponding clamped-free and free-free beams are similar in the sense that the geometric boundary conditions (deflections, rotation, and slope) are exactly satisfied while the natural boundary conditions (equilibrium conditions) are only approximately satisfied (Ref. 5). The ramifications of only approximately satisfying the natural boundary conditions will be discussed later.

Referring to Figure 3.1, let the plate's normal deflection with respect to the spanwise direction, x, (clamped-free boundary conditions) be represented by

$$W_x(x) = \sum_{i=1}^P A_i X_i(x) \quad (3.1)$$

where i - mode shape number

X_i - i -th natural mode shape for a clamped-free beam

A_i - modal weighting coefficient for mode i .

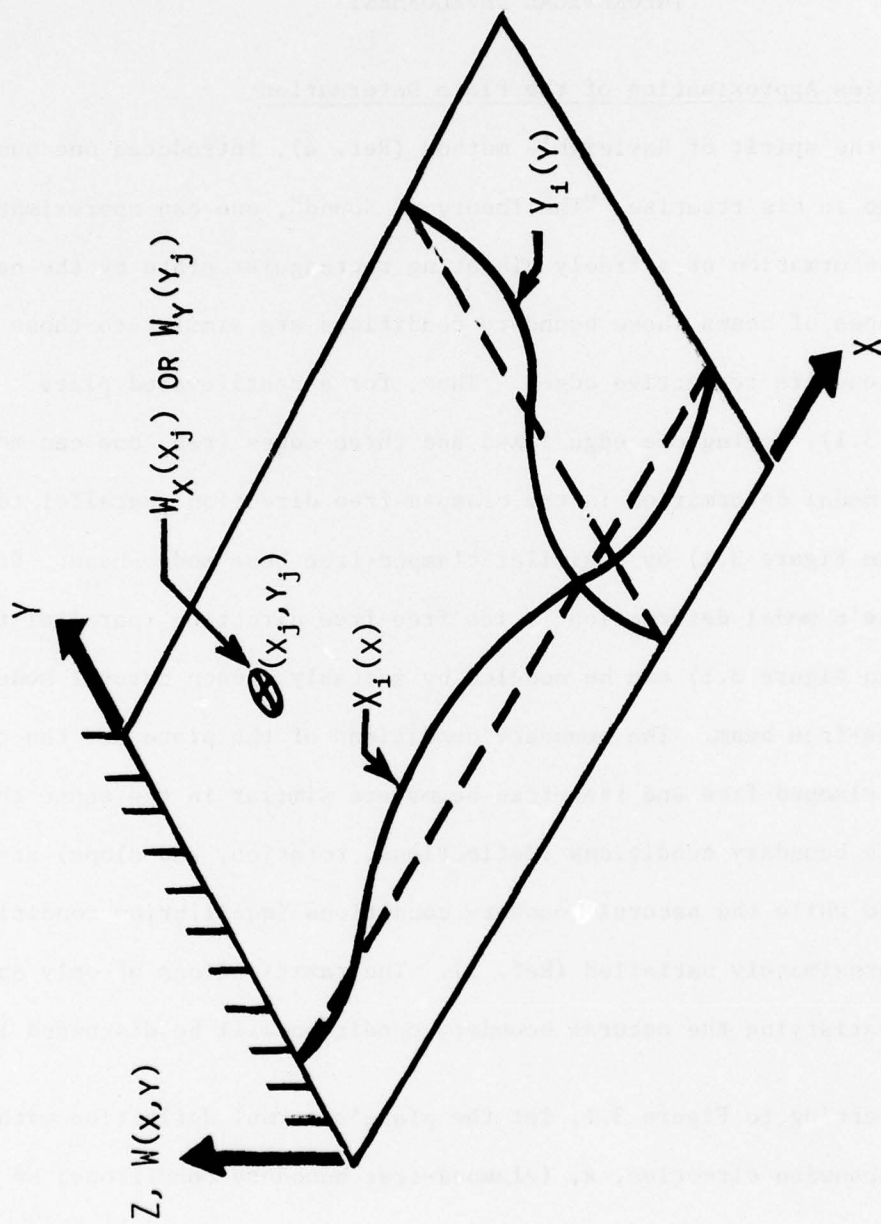


Figure 3.1 - Coordinate System for Cantilever Plate

For a beam of length, a , clamped at $x=0$ and free at $x=a$, the natural mode shapes are given by the expression (Ref. 6):

$$X_i(x) = \cosh \frac{\lambda_i x}{a} - \cos \frac{\lambda_i x}{a} - \alpha_i \left[\sinh \frac{\lambda_i x}{a} - \sin \frac{\lambda_i x}{a} \right] \quad (3.2)$$

for $i=1, 2, 3 \dots$

where λ_i - eigenvalue for the i -th mode of a clamped-free beam

α_i - constant dependent upon the mode number and boundary conditions.

The i -th eigenvalue, λ_i , is related to the beam properties by

$$\lambda_i = \left(\frac{\rho A L^4}{EI} \right)^{\frac{1}{4}} \omega_i$$

where ρ is the beam's mass density, A is the cross-sectional area of the beam, L is the beam length, E is Young's Modulus, I is the cross-sectional moment of inertia and ω_i is the i -th natural frequency of the beam.

Table 3.1 gives the eigenvalues, λ_i , and constants, α_i , for a clamped-free beam.

TABLE 3.1

Clamped-Free Beam Constants (Ref. 6)

i	λ_i	α_i
1	1.8751	.7340
2	4.6940	1.0184
3	7.8547	.9992
4	10.9955	1.0000
5	14.1371	.9999
6	17.2787	1.0
$i > 6$	$\left(\frac{2i-1}{2} \right) \pi$	1.0

Referring once more to Figure 3.1, let the plate's normal deflection with respect to the chordwise direction, y , (free-free boundary conditions) be represented by:

$$W_y(y) = \sum_{i=1}^q B_i Y_i(y) \quad (3.3)$$

where i - mode shape number

Y_i - i -th natural mode shape for a free-free beam

B_i - modal weighting coefficient for mode i

For a beam of length, b , having free boundary conditions at $y=0$ and $y=b$, the natural mode shapes are given by the following expressions (Ref. 6):

$$Y_1 = 1 \quad (3.4)$$

$$Y_2 = \sqrt{3} \left(1 - \frac{2y}{b} \right) \quad (3.5)$$

$$Y_i(y) = \cosh \frac{\gamma_i y}{b} + \cos \frac{\gamma_i y}{b} - \beta_i \left[\sinh \frac{\gamma_i y}{b} + \sin \frac{\gamma_i y}{b} \right] \quad (3.6)$$

for $i = 3, 4, 5 \dots$

where γ_i - eigenvalue for the i -th mode shape of a free-free beam

β_i - constant dependent upon the mode number and boundary conditions.

The eigenvalue, γ_i , is related to the free-free beam properties in the same way as λ_i was for a clamped-free beam. Table 3.2 gives the eigenvalues, γ_i , and constant, β_i , for a free-free beam.

TABLE 3.2

Free-Free Beam Constants (Ref. 6)

i	γ_i	β_i
3	4.7300	.9825
4	7.8532	1.0007
5	10.9956	.9999
6	14.1371	1.0000
$N > 7$	$\frac{(2N-3)\pi}{2}$	1.0

Note that the expressions given by equations (3.4) and (3.5) represent rigid body modes of the free-free beam. Equation (3.4) is a normalized translation of the beam in the z direction and equation (3.5) represents a rotation of the free-free beam about its midpoint, the vector of rotation being parallel to the x axis.

The modal functions given by equation (3.2) for the clamped-free beam and by equations (3.4) - (3.6) for the free-free beam are continuous with respect to each function's spatial variable and, hence, can be differentiated twice. Thus, from equation (3.1), the plate curvature in the x direction can be represented by

$$w_x''(x) = \sum_{i=1}^p A_i X_i''(x), \quad i = 1, 2, 3, \dots, p \quad (3.7)$$

where primes denote differentiation with respect to x . The second derivative of the i -th clamped-free mode is given by

$$X_i''(x) = \left(\frac{\lambda_i}{a}\right)^2 \left[\cosh \frac{\lambda_i x}{a} + \cos \frac{\lambda_i x}{a} - \alpha_i \left(\sinh \frac{\lambda_i x}{a} + \sin \frac{\lambda_i x}{a} \right) \right] \quad (3.8)$$

for $i=1, 2, 3 \dots$

Similarly, the plate curvature in the y direction can be represented by

$$w_y''(y) = \sum_{i=1}^q B_i Y_i''(y), \quad i = 1, 2, 3, \dots, q \quad (3.9)$$

where the second derivative of the i-th free-free mode is given by

$$Y_i''(y) = 0, \quad \text{for } i = 1, 2 \quad (3.10)$$

$$Y_i''(y) = \left(\frac{\gamma_i}{b}\right)^2 \left[\cosh \frac{\gamma_i y}{b} - \cos \frac{\gamma_i y}{b} - \beta_i \left(\sinh \frac{\gamma_i y}{b} - \sin \frac{\gamma_i y}{b} \right) \right] \quad (3.11)$$

for $i = 3, 4, 5, \dots$

Neglecting in-plane stretching, equations (3.7) and (3.9) can be used to determine the bending strains in the plate caused by the out of plane deformation. For a plate undergoing pure bending, the strains can be obtained from (Ref. 5):

$$\epsilon_x = -z w_x''(x) \quad (3.12)$$

$$\epsilon_y = -z w_y''(y) \quad (3.13)$$

where z is the perpendicular distance from the plate's neutral surface to the point of interest on the plate's surface. Note that for a twisted plate-like structure such as a compressor blade, the distance, z , does not necessarily equal half the plate thickness. Using equations (3.7) and (3.9), equations (3.12) and (3.13) can be written as:

$$\epsilon_x = -z \sum_{i=1}^p A_i X_i''(x) \quad (3.14)$$

$$\epsilon_y = -z \sum_{i=1}^q B_i Y_i''(y) \quad (3.15)$$

Looking at equations (3.14) and (3.15), we see that the normal strain with respect to x (y held constant, i.e., constant chord location for a blade) or the normal strain with respect to y (x held constant, i.e., constant span location for a blade) can be computed provided that one can arrive at suitable values for the A_i 's and B_i 's. What follows is a way of accurately computing the A_i 's and B_i 's for a specified natural mode of vibration of a plate-like structure by utilizing the interference fringes from time average laser holography.

3.2 Determination of the Model Weighting Coefficients, A_i and B_i

The weighting coefficients, A_i and B_i , that appear in equations (3.1) and (3.3) for approximating the plate deformation and also in equations (3.7) and (3.9) for approximating the plate curvature can be determined using a least squares technique based on discrete displacement data points obtained by laser holographic interferometry. For a plate-like structure vibrating in one of its natural modes of vibration, time average holographic interferometry can be used to determine the modal deformation of the structure (Ref. 7). The modal deformation is characterized by a "contour map" of fringes appearing on the surface of the plate-like structure when the time average hologram is reconstructed with laser light. A photograph of one such reconstruction is shown in Figure 3.2 which shows a turbine blade vibrating in one of its natural modes of vibration. The fringes on the blade surface are a contour map of the blade's displacement normal to the plane of the hologram. The brightest fringes are nodal lines (zero displacement) for the particular mode of vibration. As one travels away from a nodal line, the dark fringes represent increasing values of



Figure 3.2 - Holographic Interferogram of a Turbine Blade Vibrating
in a Torsional Mode at 25,943 Hz

the normal displacement and are approximately equal to integer multiples of one-quarter wavelength of the laser light. The actual value of the normal displacement of the i -th dark fringe is given by the expression (Ref. 7):

$$W_i = \frac{\Lambda \Omega_i}{2\pi(\cos \theta_1 + \theta_2)} \quad (3.16)$$

where Λ - wavelength of the laser light used to make the hologram

θ_1 - angle between the displacement vector of the plate and the line of sight of the observer/camera through the hologram

θ_2 - angle between the displacement vector of the plate and the laser "object" beam illuminating the plate

Ω_i - i -th root of the zero order Bessel function corresponding to fringe i .

If the specimen to be tested is positioned such that its principal plane of vibration is parallel to the plane of the hologram, and, in addition, is located such that its distance from the hologram is greater than five times its largest in-plane dimension, the value of θ_1 , can be made very small and $\cos \theta_1 \approx 1$. Further, if the object beam for illuminating the test specimen is placed very close to the hologram and the 5 to 1 ratio (distance of specimen from hologram to maximum specimen dimension) mentioned above is in effect, then θ_2 can also be made very small and $\cos \theta_2 \approx 1$. With these criteria placed on experimental setup, equation (3.16) takes the form

$$W_i = \frac{\Lambda \Omega_i}{4\pi} \quad (3.17)$$

Table 3.3 gives the normal displacement for the first twenty interference fringes based on the above simplifying assumptions and a laser wavelength for a HeNe laser of $\lambda = 6328\text{\AA} = 24.914 \mu\text{in}$ (Ref. 8).

TABLE 3.3

Normal Displacement Values from Holographic Fringes (Ref. 8)

Fringe Order, i	i -th Root of $J_0 (\Omega_i)$	Displacement (μin)
1	2.405	4.768
2	5.520	10.94
3	8.634	17.12
4	11.79	23.37
5	14.93	29.60
6	18.07	35.82
6	21.21	42.06
8	24.35	48.29
9	27.49	54.51
10	30.64	60.74
11	33.78	66.97
12	36.92	73.20
13	40.06	79.43
14	43.20	85.66
15	46.34	91.89
16	48.48	98.11
17	52.62	104.3
18	55.77	110.6
19	58.91	116.8
20	62.05	123.0

Utilizing equation (3.1), the experimental normal displacements, w_j , at the locations, x_j , $j = 1, 2, 3, \dots, k$, in the clamped-free direction can be set equal to the series approximation for the same deformation given by equation (3.17). In this case, the chord location, y , is held constant. Doing so, yields

$$w_x(x_j) = w_j = \sum_{i=1}^p A_i X_i(x_j), \quad j = 1, 2, \dots, k \quad (k \geq p) \quad (3.18)$$

The only unknowns in equation (3.18) are the modal weighting coefficients, A_i .

Since we require that $k > p$, equation (3.18) represents a set of k non-homogeneous simultaneous equations in p unknowns, i.e., the modal weighting coefficients, A_i , $i = 1, 2, \dots, p$. Equation (3.18) can be represented in terms of matrix notation as

$$[X] (A) = (W) \quad (3.19)$$

where $[X]$ - rectangular $k \times p$ matrix of the p clamped-free beam mode functions at the k spanwise locations,

x_j , $j=1,2,\dots,k$.

($[X]$ has rank $r \leq p$)

(A) - column vector of the p modal weighting coefficients, A_i , $i=1,2,\dots,p$.

(W) - column vector of the k normal displacements, w_j , $j=1,2,\dots,k$, obtained at the locations x_j using holographic interferometry.

For the case of $k=p$, equation (3.19) can be solved for the modal weighting coefficients, (A), using standard matrix inversion techniques. But since we are dealing with data points determined experimentally and the resulting inherent error, it is prudent to choose $k > p$ such that equation (3.19) represents an overdetermined set of equations. A "best fit" approximation for the p weighting coefficients, (A) can then be found based on the k normal displacement values, (W). This type of approach was implemented using a linear least square solution of equation (3.18) as described in the following.

The k simultaneous linear equations given by equation (3.18) can be solved for the p modal weighting coefficients, (A) , for the case of $k > p$ by utilizing the concept of the pseudoinverse developed by E. H. Moore (Ref. 9) and R. Penrose (Ref. 10) independently of each other under the name "generalized inverse". At present, the name "pseudo-inverse" is the more generally accepted term and will be used in the following discussion. The application of the pseudoinverse to the solution of overdetermined systems of linear equations is dealt with quite lucidly by Golub and Reinsch (Ref. 11).

The rectangular ($k \times p$) matrix, $[X]$, appearing in equation (3.19) can be represented as (Ref. 11)*

$$[X] = [U] [\Sigma] [V]^T \quad (3.20)$$

where $[U]$ - matrix of the p orthonormalized eigenvectors of

$$[X] [X]^T \text{ based on the } p \text{ largest eigenvalues of } [X] [X]^T$$

$[V]$ - matrix of the p orthonormalized eigenvectors of $[X]^T [X]$

$[\Sigma]$ - $\text{Diag} (\lambda_1, \lambda_2, \dots)$ is the diagonal matrix consisting of the non-negative square roots of the eigenvalues of $[X]^T [X]$.

$[\Sigma]$ is arranged such that $\lambda_1 > \lambda_2 > \dots \lambda_p$

$$[U]^T [U] = [V]^T [V] = [V] [V]^T = I_p \text{ (} I_p \text{ is the identity matrix)}$$

* $[V]^T$ - Transpose of matrix $[V]$.

The pseudoinverse of $[X]$, denoted as $[X]^+$, is obtained from the expression

$$[X]^+ = [V] [\Sigma]^{-1} [U]^T \quad (3.21)$$

where $[U]$ and $[V]$ are defined as before and

$$[\Sigma]^{-1} = \begin{bmatrix} \frac{1}{\lambda_1} & 0 & 0 & 0 & . & . & . \\ 0 & \frac{1}{\lambda_2} & 0 & 0 & . & . & . \\ . & . & . & . & 0 & 0 & \frac{1}{\lambda_p} \end{bmatrix}$$

$$[\Sigma] [\Sigma]^{-1} = [\Sigma]^{-1} [\Sigma] = I_p$$

equation (3.21) can be used to solve for the modal weighting coefficients in equation (3.19).

Pre-multiplying by $[X]^+$ yields:

$$[X]^+ [X] (A) = [X]^+ (W) \quad (3.22)$$

$$[I_p] (A) = [X]^+ (W) \quad (3.23)$$

$$(A) = [V] [\Sigma]^{-1} [U]^T (W) \quad (3.24)$$

Equation (3.24) gives the p weighting coefficients based on the k input displacements and the p clamped-free beam functions evaluated at the locations x_j , $j=1,2,\dots,k$. The nature of this solution is indeed fortuitous for the following two reasons (Ref. 12). First, if the rank, r , of matrix $[X]$ is $r=p$, then the weighting coefficient vector (A) in equation (3.24) is the "best fit" in the sense that it is nearest to the actual vector (A) in a least squares sense. Second, if the rank of matrix $[X]$ is $r < p$, then there is no exact solution

but equation (3.24) still gives the best solution in the sense of least squares, i.e., $[X](A)$ is as close to (W) as possible. Appendix A gives a simple example of computing the pseudoinverse of a 3×2 matrix.

The computation of the pseudoinverse of $[X]$ in equation (3.19) and the resulting solution for the modal weighting coefficients, (A) , was carried out using the computer program LLSQAR that is on permanent file on the computer system at Wright-Patterson AFB. The routine is part of the Computer Science Center's International Mathematical Scientific Library package. A brief description on the actual mechanics of using LLSQAR is given in Appendix D.

With the values of the modal weighting coefficients determined, equations (3.1) and (3.7) can be used to determine the displacement and curvature, respectively, for any location, x , $y = \text{constant}$, along the span of the plate.

In a manner exactly paralleling the preceding development for plate deformation based on a fixed-free modal series, the modal weighting coefficients appearing in equation (3.3) for a free-free beam series can be determined by using the experimental normal displacements, w_j , at each of k locations, y_j , $j=1,2,3,\dots,k$, in a line across the chord of the plate, in the free-free direction. In this case, the span or x location of the plate will be held constant. Carrying this out, yields the equation

$$w_y(y) = w_j = \sum_{i=1}^q B_i Y_i(y_j) \quad (3.25)$$

for $i=1,2,\dots,q$ and $j=1,2,\dots,k$ ($k \geq q$)

The modal weighting coefficients, B_1 , are then computed using the computer algorithm LLSQAR. Once this has been accomplished, the displacement and curvature at any point y , $x=\text{constant}$, can be computed via equations (3.3) and (3.9). Section IV of this report presents a detailed discussion of the steps involved in applying the method to a typical plate vibration mode shape.

3.3 Ramifications of Using Simple Beam Eigenfunctions

At the beginning of this section mention was made of the fact that while the clamped-free and free-free beam functions satisfy the corresponding plate geometric boundary conditions exactly, the plate's natural boundary conditions along its free edges are only approximately satisfied. The ramifications of this can be seen by looking at the natural boundary conditions that must be satisfied along the tip of the cantiliver plate shown in Figure 3.1. Satisfying equilibrium along this edge requires that the shear forces in the x direction and the moments about the y axis be zero. Hence, we require that:

$$M_x \Big|_{x=a} = D \left(\frac{\partial^2 W}{\partial x^2} + \nu \frac{\partial^2 W}{\partial y^2} \right) \Big|_{x=a} = 0 \quad (3.26)$$

$$V_x \Big|_{x=a} = D \left[\frac{\partial^3 W}{\partial x^3} + (2 - \nu) \frac{\partial^3 W}{\partial x \partial y^2} \right] \Big|_{x=a} = 0 \quad (3.27)$$

where $D = \frac{Eh^3}{12(1-\nu^2)}$ is the plate flexural stiffness. Now the clamped-free beam function given by equation (3.2) has the property that the first term in each of equations (3.26) and (3.27) is identically equal to zero, i.e.,

$$\frac{\partial^2 W}{\partial x^2} = \frac{\partial^3 W}{\partial x^3} = 0, \quad x = a \quad (3.28)$$

when $W(x)$ is approximated by a series of clamped-free beam functions.

This means that the calculated moment and, hence the strain, ϵ_x , at

the plate free edge will have an error that is proportional to

$y \frac{\delta^2 W}{\delta y^2}$ and the calculated shear will have an error that is proportional to $(2-\nu) \frac{\delta^3 W}{\delta x \delta y^2}$. There will be a similar error in the value of the chord-

wise strain, ϵ_y , at the plate's free edges $y=0$ and b . Fortunately, the

magnitude of this inherent error is not appreciable as will be seen in

Section IV.

SECTION IV

INTERACTIVE COMPUTER PROGRAM - HOLOCURVE

The technique developed in Section III for determining the displacement and curvature of a vibrating plate-like structure was programmed for use on a CDC6600 computer via a Tektronix 4010 interactive computer terminal. By using the Tektronix computer unit, one has the advantage of interacting with the computer program while it is executing on the CDC6600 computer. In this way, input data can be deleted or modified, decisions as to program direction can be made, and, most importantly, the results are returned to the user immediately in either tabular or plot format.

Figure 4.1 shows a flow chart of the computer program called HOLOCURVE. A listing of the program is given in Appendix B. The questions that the user must answer while executing HOLOCURVE are listed below in order of appearance on the Tektronix 4010 screen along with possible answers (in brackets) and a brief discussion of each entry.

1. WHAT IS THE MODE NAME (8H)? - - -

Input any letter/number identifier that takes up eight spaces or less.

2. WILL OUTPUT BE BASED ON CLAMPED-FREE (CF) OR FREE-FREE (FF) BEAM SERIES? TYPE CF OR FF. - - - [CF / FF]

Program is henceforth keyed to either a clamped-free or free-free modal beam series.

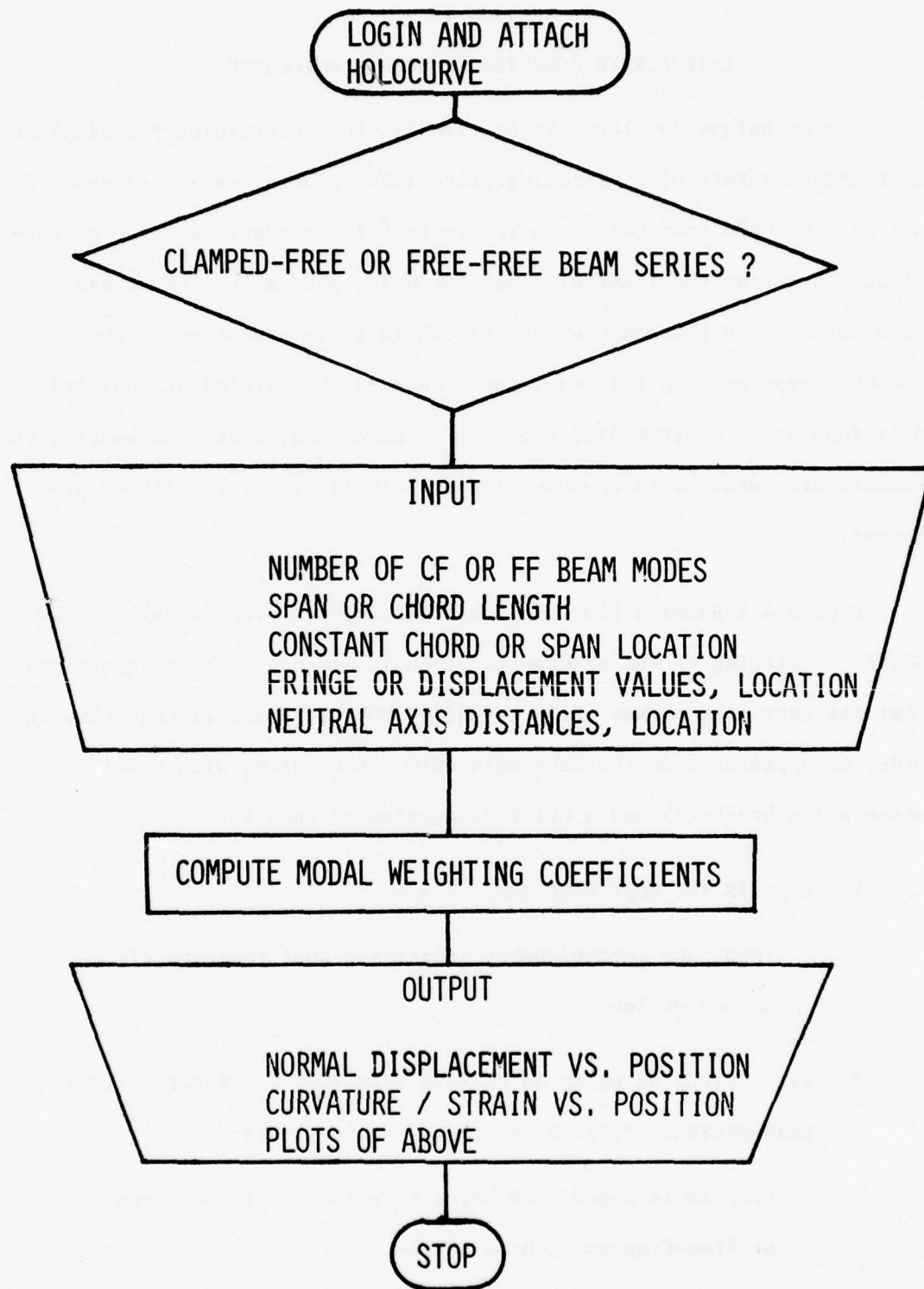


Figure 4.1 - Flow Chart for Program HOLOCURVE

3. HOW MANY CF [OR FF] BEAM SERIES TERMS WILL BE USED? - - -

[Floating point whole number]

This specifies the value of p in equation (3.1) for a clamped-free beam or of q in equation (3.3) for a free-free beam. For the lower mode shapes (first and second bending, first and second torsion, lyre or two-stripe), a value of $p = 5$ or $Q = 5$ gives adequate results.

4. INPUT NUMBER OF FRINGE VALUES. - - -

Specifies number of discrete holographic fringe value data points that will be used.

5. INPUT SPAN [OR CHORD] LENGTH. - - - [Floating point number]

For the clamped-free case, the actual length of the span segment is input. This corresponds to the beam length, a , in equation (3.2). For example, the distance from the root to the tip of a compressor blade could be entered. For the free-free case, the length of the chord segment is input. This corresponds to the beam length, b , in equations (3.5) and (3.6). It could, for example, be the distance from the leading edge to the trailing edge of a compressor blade.

6. INPUT CONSTANT CHORD (Y) [OR SPAN (X)] LOCATION. - - -

This establishes the constant y or x location on the plate or blade for the case of a clamped-free or free-free beam series approximation, respectively. (See Figure 3.1)

7. INPUT PAIRS OF SPAN [CHORD] LOCATION, FRINGE VALUE DATA.

FREE FIELD FORMAT WITH EACH VALUE SEPARATED BY COMMAS.

DATA = [1, -5., 2, -11., 3., -12., 4.1, -8, 4.94, 0., 6., 9.,
7., 16.]

Pairs of span (or chord) location vs. holographic fringe value are input. Seven such pairs of data are input in the example shown. Note that the fringe values are positive or negative whole numbers. Note, also, there is a nodal point at $x = 4.94$ where the fringe value is given as zero. The HOLOCURVE subroutine, CONVRT, converts the fringe values to normal displacements using the expression given in equation (3.17).

8. WILL DISTANCE FROM NEUTRAL AXIS VS. SPAN [OR CHORD] LOCATION

BE INPUT - YES OR NO? - - -

If "YES", the following two statements must be answered:

HOW MANY (SEGMENT LOCATION/NEUTRAL AXIS DISTANCE) VALUES WILL
BE INPUT (MAX. OF 20)? - - - [5.]

INPUT 5. PAIRS OF (SEGMENT LOCATION, NEUTRAL AXIS
DISTANCE) VALUES.

DATA = [0., .25, 1., .28, 3., .30, 5., .25, 6., .20, 7., .15]

In order to compute the bending strain at a point on the plate or blade, the distance from the neutral axis must be known (see, for example, equations (3.12) and (3.13)). In the case

of a flat plate-like structure having constant thickness, this distance is merely half of the thickness. In the case of a twisted or curved plate-like body having variable thickness, however, the neutral axis distance is not so easily computed and is entered in discrete form as in the above "DATA" entry. When the bending strains are computed along the span or chord section being analyzed, a subroutine (INTERP) utilizes a second degree polynomial interpolation scheme to compute the neutral axis distance based on the discrete input data. Appendix E. contains a more complete description of subroutine INTERP.

9. DO YOU WISH TO SEE INPUT DATA (YES OR NO)? - - -

A listing of fringe values and their location, and, if used, neutral axis distance values and their location are displayed.

10. COMPUTATION COMPLETED FOR [Mode Name] MODE, DATA SET = 1. DO YOU WISH TO SEE MODAL WEIGHTING COEFFICIENTS FOR THE CF[OR FF] BEAM SERIES - YES OR NO? - - -

An affirmative answer yields a listing of the modal weighting coefficients given in equations (3.1) or (3.3).

11. DISPLACEMENT AND CURVATURE AS A FUNCTION OF POSITION WILL NOW BE LISTED AND PLOTTED FOR MODE [Mode Name].

HOW MANY DATA POINTS DO YOU WANT (MAX. OF 40)? - - -

Chord or span segment is evenly divided into number of data points entered. Program then proceeds to give a listing of

the normal displacement as a function of position and a plot of same. It then gives a listing of the curvature (bending strain) as a function of position, and an accompanying plot.

12. IS THERE MORE DATA TO BE ANALYZED (YES OR NO?) - - -

If answer is affirmative, cycle of questions is repeated;
if negative, HOLOCURVE completes its execution and user may
"LOG OFF" from terminal.

Appendix C. gives a typical example of the above statements being used during a HOLOCURVE execution.

SECTION V

DISPLACEMENT AND STRAIN DETERMINATION USING HOLOCURVE

5.1 Displacement and Strain Distribution of a Vibrating Plate

In order to check the effectiveness and accuracy of the holographic data reduction technique utilized by HOLOCURVE, three natural modes of vibration of a cantilevered flat plate were determined using holographic interferometry and the resulting fringe data was input to HOLOCURVE to determine the displacement and bending strain at selected locations for each of the three vibration modes. The results from this analysis were compared to those of an eigenvalue analysis carried out on a finite element model of the plate using the multi-purpose finite element computer program, NASTRAN (Rigid Format 3).

The plate was made of 6061-T6 Aluminum and measured 3" by 7" with a thickness of .19". It was fixed along one of its short sides by clamping it between two massive steel blocks. Time average holograms were made of each of the three natural plate modes of vibration while the plate was being excited by a 40-watt siren. A schematic of the holographic set-up is shown in Figure 5.1. The set-up is quite typical of the type used for doing holographic interferometry. A 50mw continuous wave HeNe laser (Spectra-Physics 125A) was used for the tests with the holograms being recorded on 4"x5" photographic plates (Agfa-Gevaert 10E75).

What follows are the results of using HOLOCURVE to get the displacement and corresponding bending strain for the plate vibration modes--second bending, second torsion, and the lyre mode.

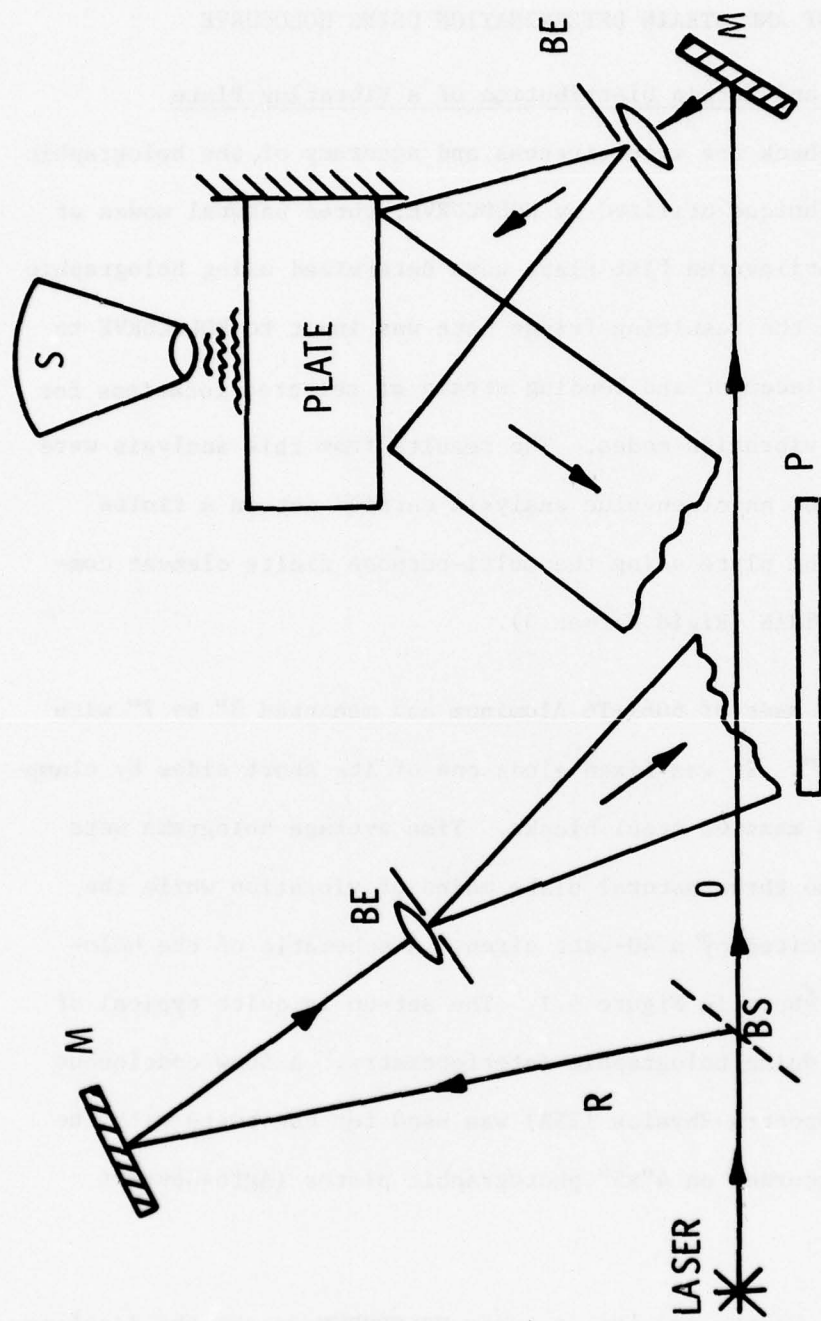


Figure 5.1 - Schematic of Experimental Set-up; BS-beam splitter, M-mirror, BE-beam expander, P-photographic plate, S-siren, R-reference beam, O-object beam

5.2 Lyre Mode of Vibration

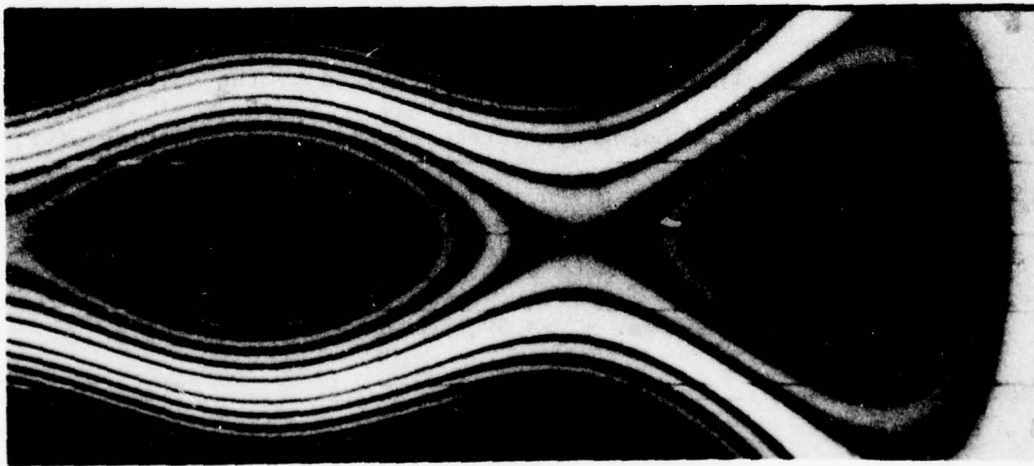
Figure 5.2 shows the lyre mode (after the Greek instrument) of the cantilever plate obtained using holographic interferometry and finite element analysis. Note that the natural frequencies determined by each of the techniques differ by only 1.2%. In the figure, the plate is clamped along its bottom edge. The lyre mode, or a form similar to it, is a common one in turbine engine compressor blading.

Referring to Figure 5.2, let a Cartesian coordinate system originate at the lower right-hand corner of the plate with the x axis lying along the plate's right edge and the y axis lying along the bottom (fixed) edge of the plate. Using this coordinate system, the displacement and corresponding bending strain were determined with respect to the x coordinate (spanwise direction) while keeping y (the chordwise direction) constant at $y=.5$ ". Note that the coordinate system just defined is the same as the one shown in Figure 3.1 of Section III, Theoretical Development.

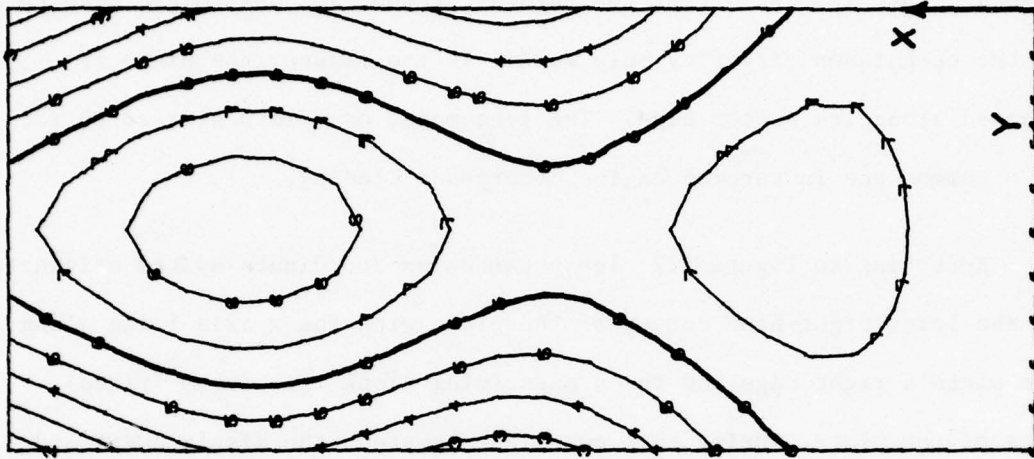
Referring to the lyre mode shape characterized by the holographic fringes in Figure 5.2, the holographic fringe values as a function of x, $y=.5$ ", were determined and are given in Table 5.1.

TABLE 5.1
Fringe Values vs. x, $y=.5$ ", for Lyre Mode

Fringe Number, N	Span Location, x, (in.)	Fringe Value, F
1	.50	1
2	1.25	2
3	2.50	-2
4	3.50	-4
5	4.30	-2
6	5.32	0
7	6.25	-2
8	6.95	-5



Experimental, $f = 4583$ Hz



Finite Element, $f = 4529$ Hz

Figure 5.2 - Lyre Mode of Vibration for Cantilever Plate

The fringe values and span locations given in Table 5.1 are not the complete set of values occurring on this spanwise segment of the plate and, hence, Table 5.1 does not represent a unique set of fringe value data for the span. Some general rules of thumb were used, however, in their choice.

1. Fringe value locations should be chosen such that they are approximately evenly spaced over the segment length.
2. The total number of fringe values used must be greater than the number of beam series functions input to HOLOCURVE. This will insure that full advantage is taken of the "smoothing" characteristics of the linear least squares subroutine, LLSQAR.
3. When possible, specify the locations of the nodal lines with the exception of the clamped end nodal line in the case of the clamped-free beam series approximation. To do so in this latter instance would be redundant since zero displacement is one of the geometric boundary conditions of the clamped-free beam functions.
4. Finally, regarding the number of beam functions specified for HOLOCURVE, in the case of clamped-free beam series approximation, the number of beam series functions used should be greater than or equal to the number of node lines crossing the span plus two, i.e.,

$$\text{Number CF Series Functions} = \text{Number Node Lines} + 2.$$

For the case of a free-free beam series approximation, the number of beam series functions used should be greater than or equal to the number of node lines crossing the chord plus three. i.e.,

$$\text{Number FF Series Functions} = \text{Number Node Lines} + 3.$$

The set of eight fringe values and their span locations given in Table 5.1 were input to HOLOCURVE where they were used to compute the modal weighting coefficients of a five-term clamped-free beam series. The computed normal displacement is shown as the smooth curve in Figure 5.3 as a function of the span, x . Also shown in the figure are the normal displacement values computed from the finite element model of the plate using NASTRAN. The finite element values were normalized to the maximum displacement at the

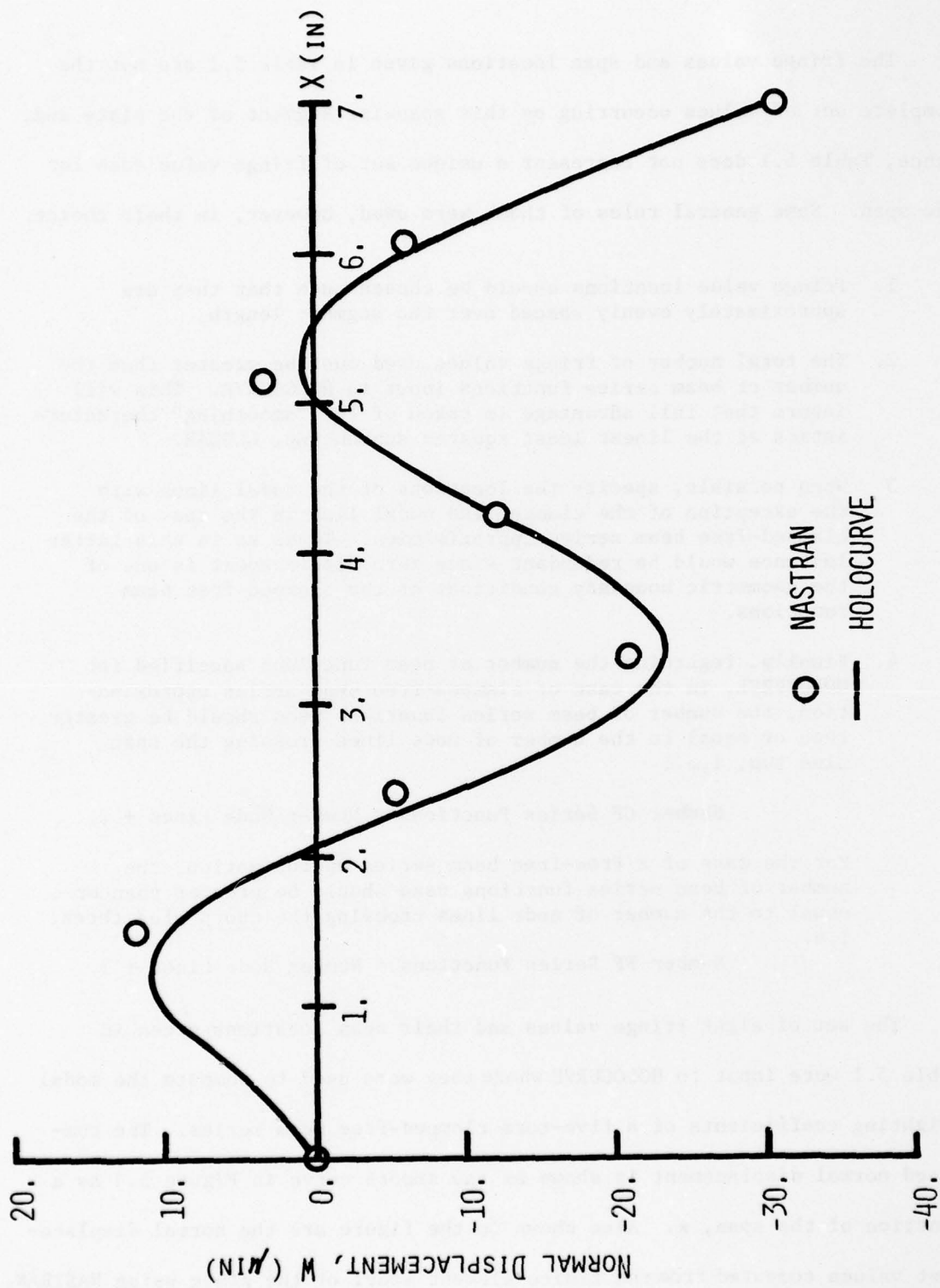


Figure 5.3 - Normal Displacement, W, vs. Span, X, at Y=5" for Lyre Mode

plate tip as determined by HOLOCURVE. It is seen that the agreement between the two methods is quite good. The modal weighting coefficients upon which the HOLOCURVE results are based are listed in Table 5.2.

TABLE 5.2

Modal Weighting Coefficient for CF Series
Approximation of Lyre Mode

CF Beam Mode, i	Modal Weighting Coefficient, $A_i \times 10^6$
1	-8.66
2	-2.860
3	-1.886
4	9.164
5	1.526

Note that coefficients A_1 , and A_4 , representing the first and fourth clamped-free beam bending mode shapes, respectively, are the dominant terms in the series. This is as one would expect, since the first order of deflection of the mode is that of a negative first bending mode while the actual modal displacement is that of a positive fourth bending mode shape, i.e., four nodal lines.

Figure 5.4 shows the resulting bending strain, ϵ_x , in the plate's x direction computed from the second derivative of the five-term clamped-free beam series. As in the plot of the normal displacement, the individual data points in the figure represent results from the NASTRAN finite element analysis of the plate.

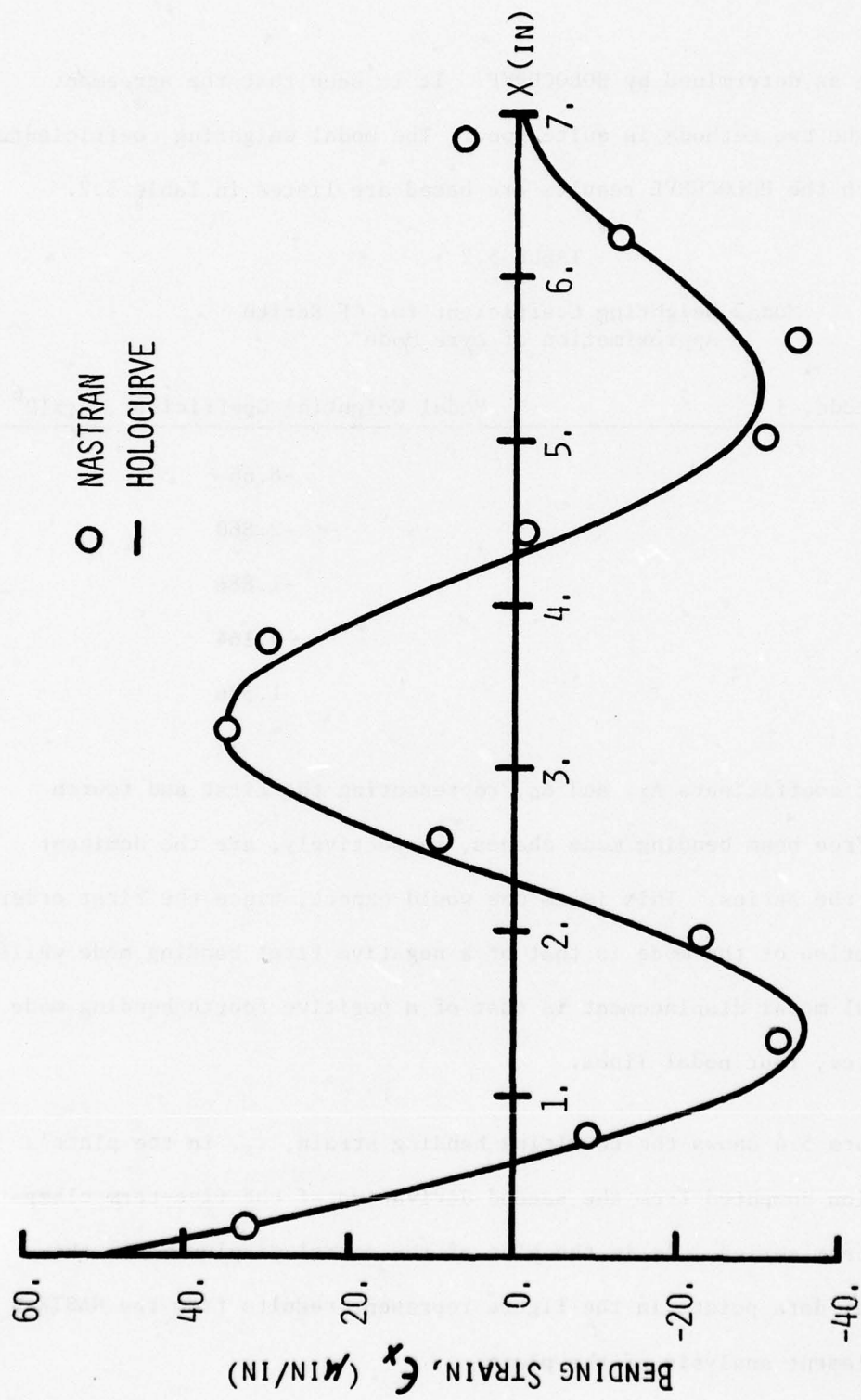


Figure 5.4 - Bending Strain, ϵ_x , vs. Span, X, at Y=.5" for Lyre Mode

The values of the bending strain, computed using NASTRAN, were normalized to the HOLOCURVE output at the span location, $x=.15''$. Again, the agreement is seen to be quite good.

The displacement and resulting bending strain were also determined for the lyre mode in Figure 5.2 as a function of the width, y , for $x=2.5''$. The holographic fringes upon which the HOLOCURVE computations were based are given in Table 5.3.

TABLE 5.3

Fringe Values vs. y , $x=2.5''$, for Lyre Mode

Fringe Number, N	Chord Location, y (in.)	Fringe Value, F
1	.06	-5
2	.48	-2
3	.80	0
4	1.20	2
5	1.84	2
6	2.25	0
7	2.53	-2
8	2.96	-5

This set of eight fringe values and chord location data were used in HOLOCURVE to compute the modal weighting coefficients of a 5-term free-free beam series. The normal displacement curve computed from this series is shown as the smooth curve in Figure 5.5 along with the normalized grid point displacements from the NASTRAN finite element calculations. Note that the finite element computations yield a greater value for the displacement at the chord midpoint. This maximum

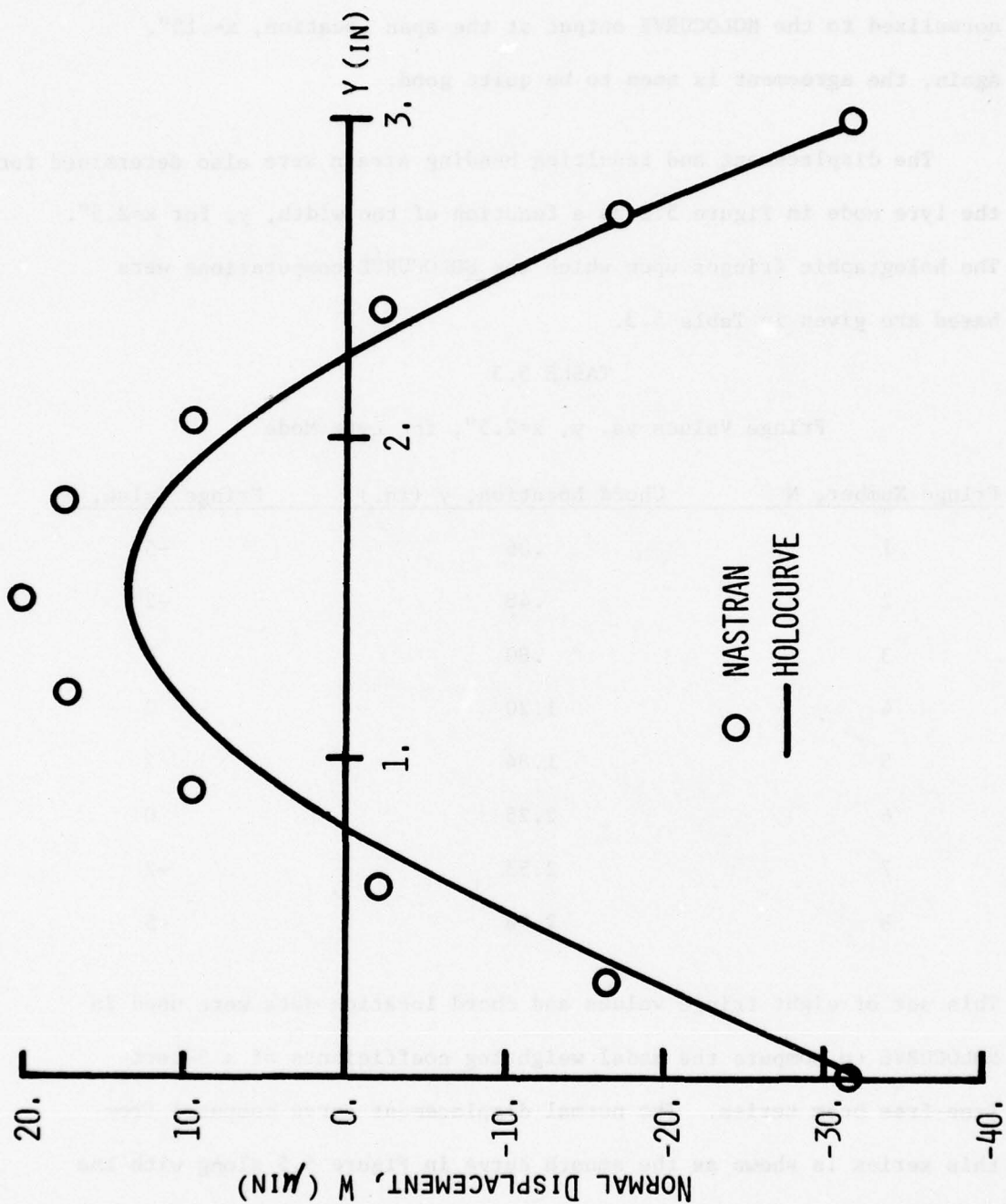


Figure 5.5 - Normal Displacement, W , vs. Chord, Y , at $X=2.5$ " for Lyre Mode

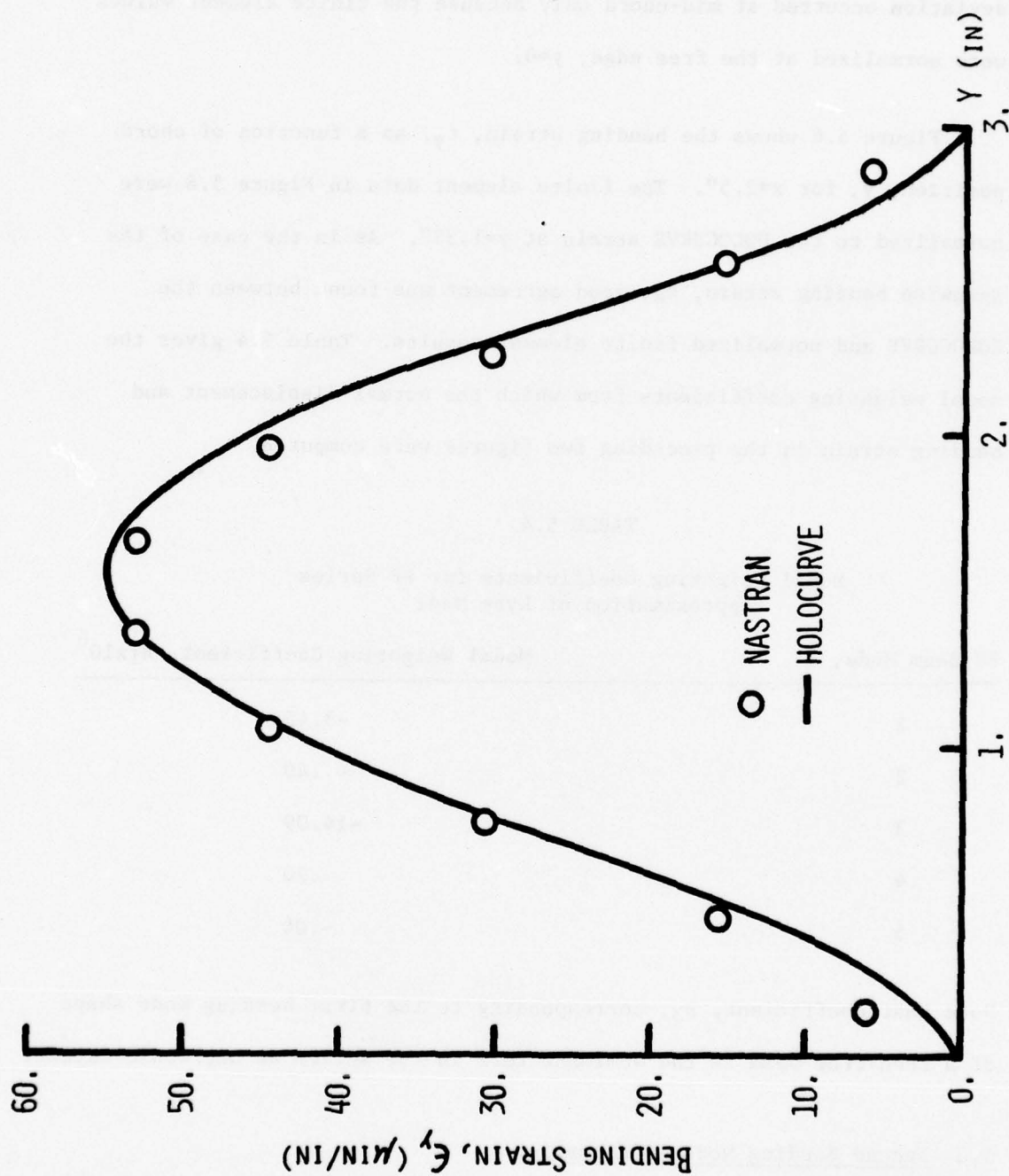


Figure 5.6 - Bending Strain, ϵ_y , vs. Chord, Y, at X=2.5" for Lyre Mode

deviation occurred at mid-chord only because the finite element values were normalized at the free edge, $y=0$.

Figure 5.6 shows the bending strain, ϵ_y , as a function of chord position, y , for $x=2.5$ ". The finite element data in Figure 5.6 were normalized to the HOLOCURVE strain at $y=1.35$ ". As in the case of the spanwise bending strain, ϵ_x , good agreement was found between the HOLOCURVE and normalized finite element results. Table 5.4 gives the modal weighting coefficients from which the normal displacement and bending strain in the preceding two figures were computed.

TABLE 5.4

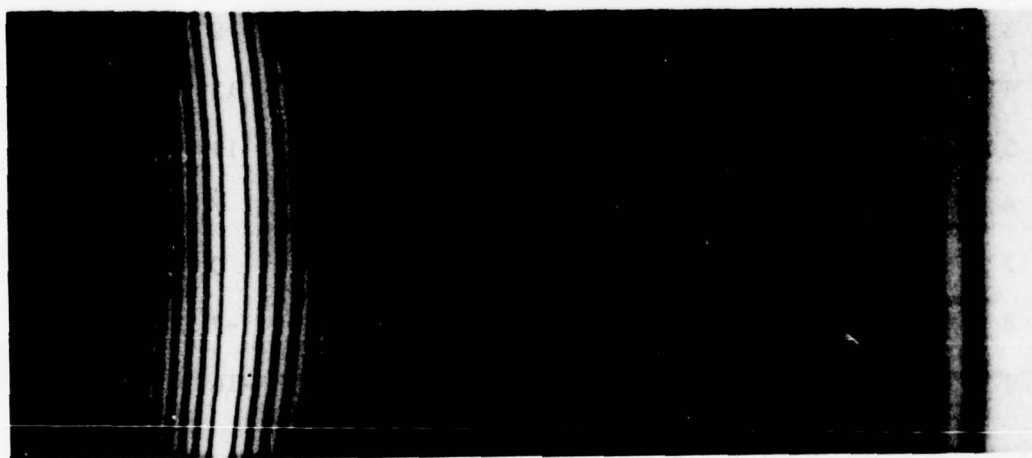
Modal Weighting Coefficients for FF Series
Approximation of Lyre Mode

FF Beam Mode, i	Modal Weighting Coefficient, $B_i \times 10^6$
1	-3.45
2	-.40
3	-14.09
4	.20
5	-.04

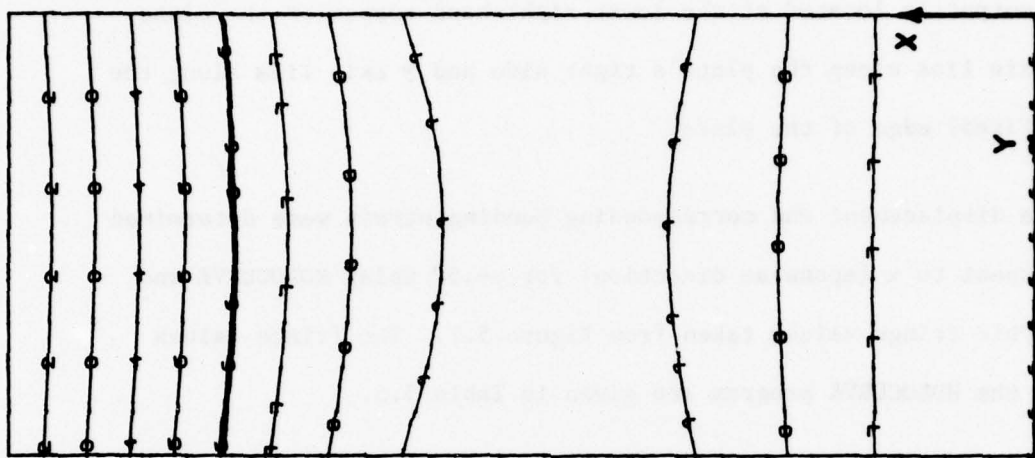
Note that coefficient, B_3 , corresponding to the first bending mode shape of a free-free beam is the dominant term in the series as one would expect.

5.3 Second Bending Mode of Vibration

Figure 5.7 shows the second bending mode of vibration for the cantilever plate obtained using holographic interferometry and finite element



Experimental, $f = 774$ Hz



Finite Element, $f = 782$ Hz

Figure 5.7 - Second Bending Mode of Vibration for Cantilever Plate

analysis. As in the preceding section on the lyre mode, the coordinate system for locating fringe values and interpreting displacement and strain output is located at the lower right-hand corner of the plate. The x axis lies along the plate's right side and y axis lies along the lower (fixed) edge of the plate.

The displacement and corresponding bending strain were determined with respect to x (spanwise direction) for $y=.5$ " using HOLOCURVE and holographic fringe values taken from Figure 5.7. The fringe values used in the HOLOCURVE program are given in Table 5.5.

TABLE 5.5

Fringe Values vs. x, $y=.5$ ", for Second Bending Mode

Fringe Number, N	Span Location, x (in.)	Fringe Value, F
1	.44	1
2	1.16	4
3	2.11	9
4	2.66	11
5	3.88	11
6	4.66	7
7	5.44	0
8	6.11	-7
9	6.98	-16

This set of data was input to HOLOCURVE and a five-term clamped-free beam series was generated. The modal weighting coefficients for this beam series are given in Table 5.6.

TABLE 5.6

Modal Weighting Coefficients for CF Series
Approximation of Second Bending Mode

CF Beam Mode, i	Modal Weighting Coefficient, $A_i \times 10^6$
1	-.68
2	50.64
3	.83
4	-.24
5	.51

Looking at Table 5.6, it is evident that the plate's second bending mode shape is quite similar to that of a simple clamped-free beam and, hence, the modal weighting coefficient, A_2 , dominates the clamped-free beam series.

Figure 5.8 shows the plate's second bending mode normal displacement computed by HOLOCURVE as a function of the span coordinate, x , for $y=.5"$. The normal displacement values determined by finite element analysis were normalized to the HOLOCURVE displacement at the plate's free edge ($x=7.0"$). The agreement between the two methods of analysis for this case are remarkably good.

The bending strain, ϵ_x , resulting from the plate displacement shown in Figure 5.8 is shown in Figure 5.9. As in the case of the lyre mode, the bending strain values computed using the finite element method were normalized to the HOLOCURVE strain value at $x=.15"$. Again, the agreement between the two methods is seen to be quite good.

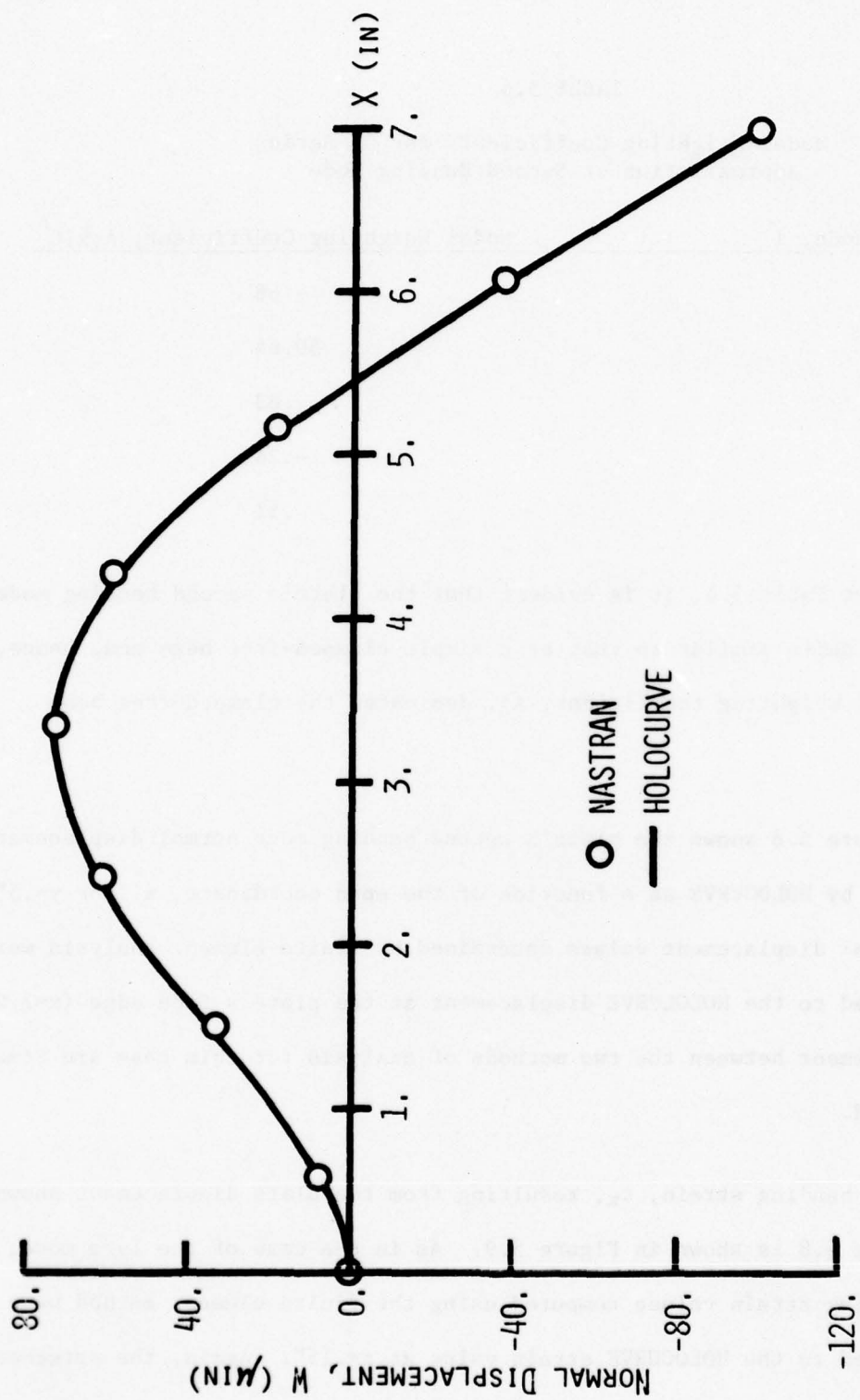


Figure 5.8 - Normal Displacement, W , vs. Span, X , at $Y = .5$ " for Second Bending Mode

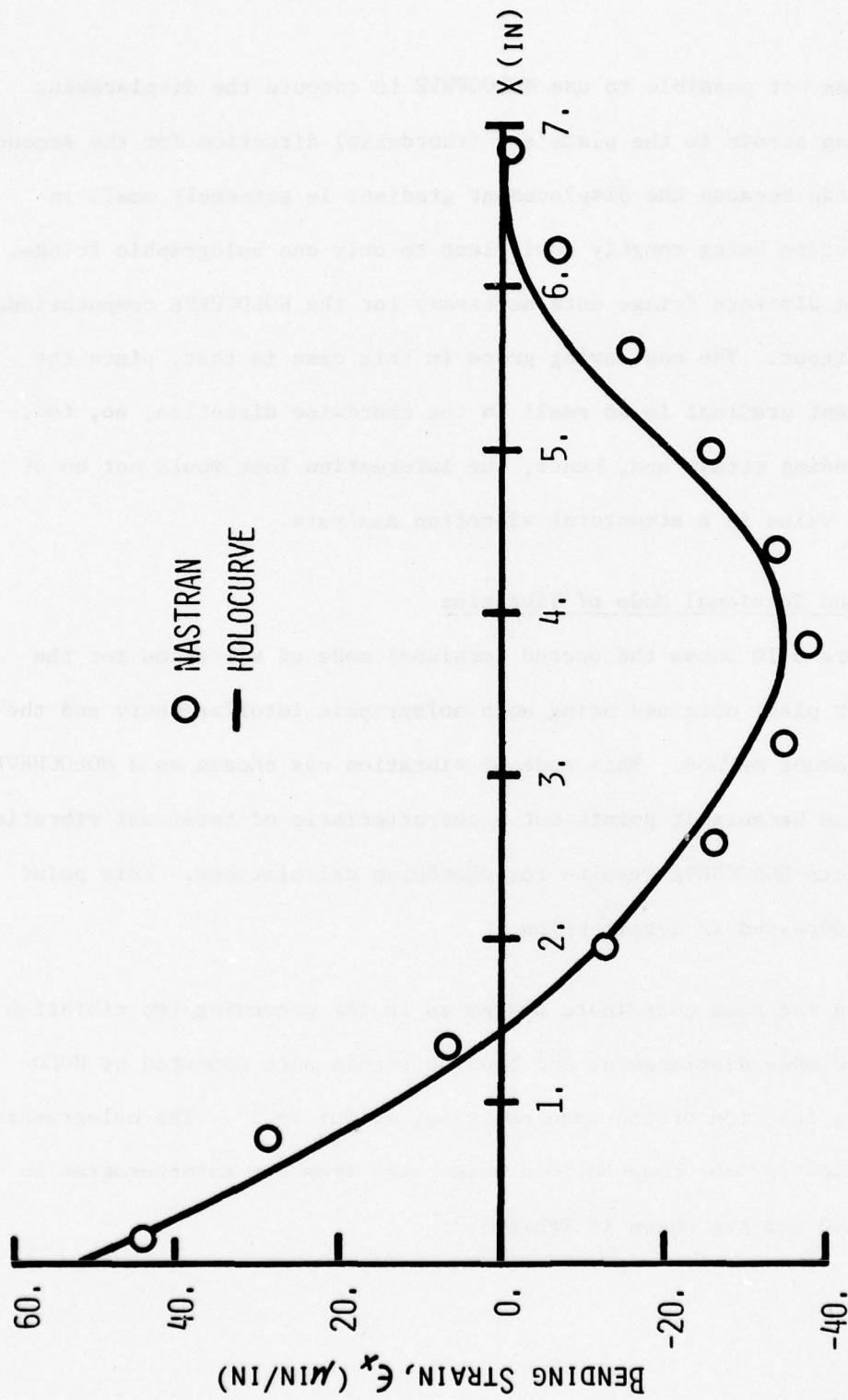


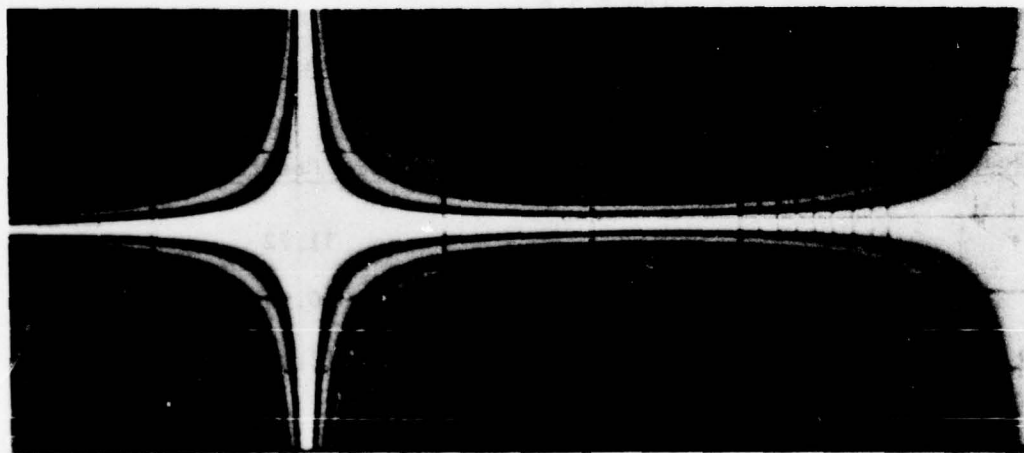
Figure 5.9 - Bending Strain, ϵ_x , vs. Span, X, at Y=.5" for Second Bending Mode

It was not possible to use HOLOCURVE to compute the displacement and bending strain in the plate's y (chordwise) direction for the second bending mode because the displacement gradient is extremely small in this direction being roughly equivalent to only one holographic fringe. Hence, the discrete fringe data necessary for the HOLOCURVE computations is nonexistent. The one saving grace in this case is that, since the displacement gradient is so small in the chordwise direction, so, too, is the bending strain and, hence, the information lost would not be of any great value in a structural vibration analysis.

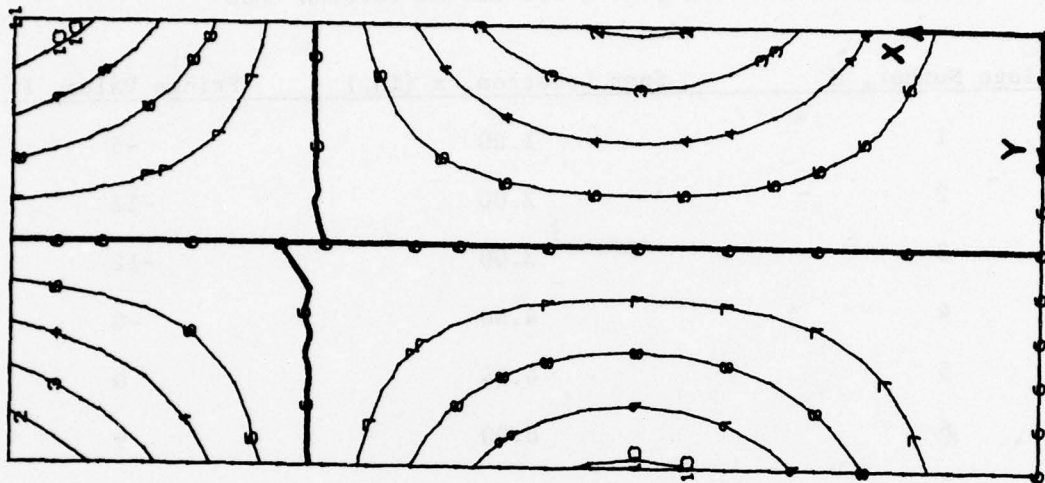
5.4 Second Torsional Mode of Vibration

Figure 5.10 shows the second torsional mode of vibration for the cantilever plate obtained using both holographic interferometry and the finite element method. This mode of vibration was chosen as a HOLOCURVE application because it points out a characteristic of torsional vibration that impacts HOLOCURVE results for chordwise calculations. This point will be addressed in detail below.

Using the same coordinate system as in the preceding two vibration modes, the mode displacement and bending strain were computed by HOLOCURVE as a function of the span position, x , for $y=.5$ ". The holographic fringes used for the computations were taken from the interferogram in Figure 5.10 and are shown in Table 5.7.



Experimental, $f = 1897$ Hz



Finite Element, $f = 1956$ Hz

Figure 5.10 - Second Torsion Mode of Vibration for Cantilever Plate

TABLE 5.7

Fringe Values vs. x , $y=.5''$, for Second Torsion Mode

Fringe Number, N	Span Location, x (in.)	Fringe Value, F
1	1.00	-5
2	2.00	-11
3	3.00	-12
4	4.00	-8
5	4.94	0
6	6.00	9
7	7.00	16

Entering this set of data into the HOLOCURVE, the modal weighting coefficients were computed for a five-term clamped-free beam series and are shown in Table 5.8.

TABLE 5.8

Modal Weighting Coefficients for CF Series
Approximation of Second Torsion Mode

CF Beam Mode, i	Modal Weighting Coefficient, $A_i \times 10^6$
1	11.72
2	-50.84
3	-12.54
4	-.46
5	-1.49

This five-term series was used to compute the normal displacement, W ,

and corresponding bending strain, ϵ_x , which are shown as the smooth curves in Figures 5.11 and 5.12, respectively. The HOLOCURVE and finite element results are again in good agreement. As in the preceding two cases, the finite element data was normalized to the HOLOCURVE displacement with respect to the plate's free end and to the HOLOCURVE bending strain at $x=.15$ ".

An analysis was also carried out using HOLOCURVE to determine the displacement and bending strain in the plate's y (chordwise) direction with $x=1.0$ ". Table 5.9 lists the holographic fringe data used in the analysis.

TABLE 5.9
Fringe Values vs. y , $x=1.0$ ", for Second Torsion Mode

Fringe Number, N	Chord Location, Y (in.)	Fringe Value, F
1	.08	-7
2	.30	-6
3	.50	-5
4	.70	-4
5	.90	-3
6	1.10	-2
7	1.32	-1
8	1.47	0
9	1.62	1
10	1.83	2
11	2.02	3
12	2.22	4
13	2.43	4
14	2.62	6
15	2.83	7
16	3.00	8

This set of fringe data differs from the others used up to this point in that all of the fringes and their corresponding chord locations at $x=1.0$ " were used.

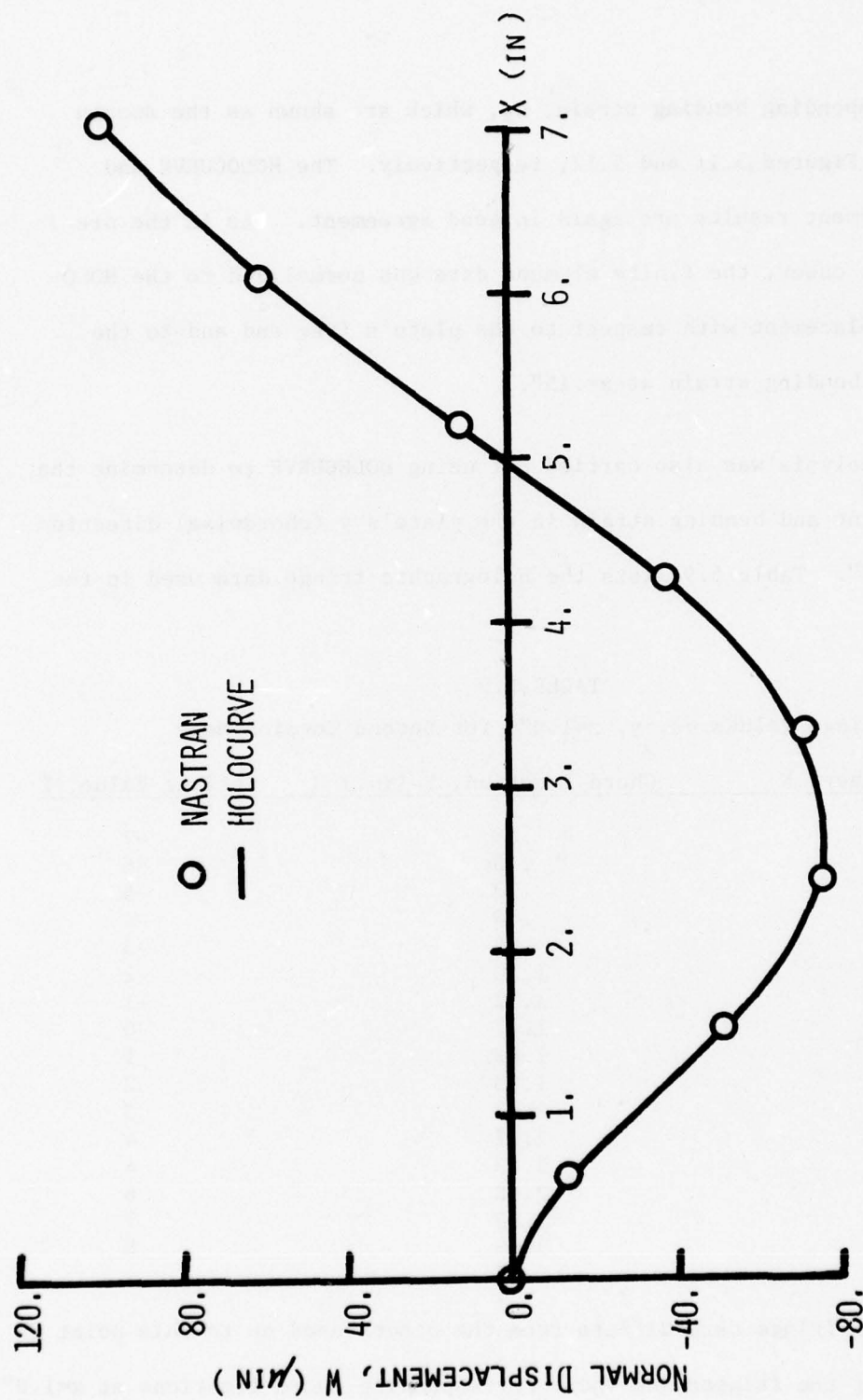


Figure 5.11 - Normal Displacement, W, vs. Span, X, at Y=.5" for Second Torsion Mode

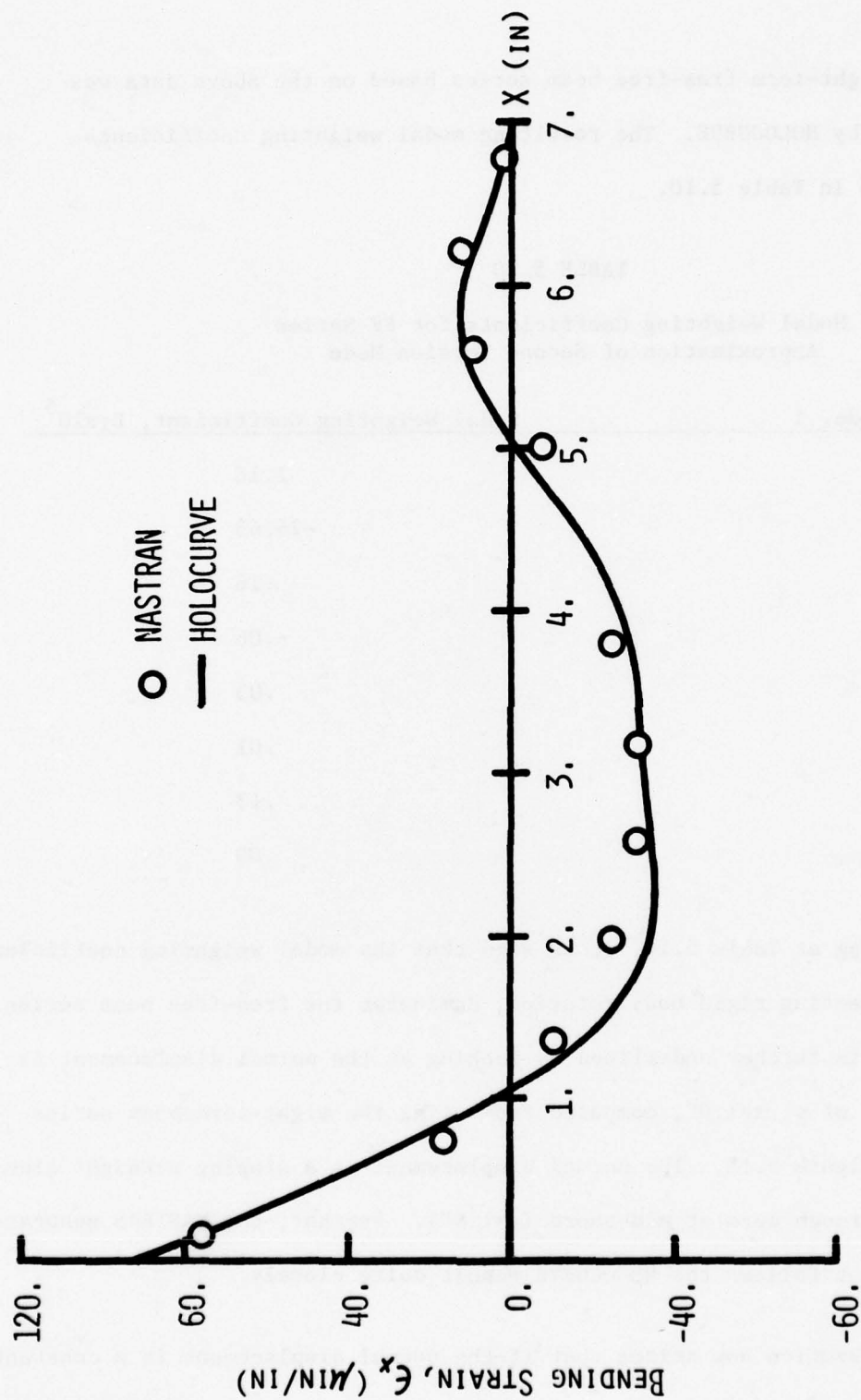


Figure 5.12 - Bending Strain, ϵ_x , vs. Span, X, at Y=5" for Second Torsion Mode

An eight-term free-free beam series based on the above data was generated by HOLOCURVE. The resulting modal weighting coefficients are listed in Table 5.10.

TABLE 5.10

Modal Weighting Coefficients for FF Series
Approximation of Second Torsion Mode

FF Beam Mode, i	Modal Weighting Coefficient, $B_i \times 10^6$
1	1.18
2	-26.63
3	.16
4	-.06
5	.03
6	.01
7	.13
8	.00

Looking at Table 5.10, it is seen that the modal weighting coefficient, B_2 , representing rigid body rotation, dominates the free-free beam series. This fact is further underlined by looking at the normal displacement as a function of y , $x=1.0''$, computed from using the eight-term beam series shown in Figure 5.13. The normal displacement is a sloping straight line passing through zero at mid-chord ($y=1.5''$). Further, the NASTRAN generated displacement follows the HOLOCURVE result quite closely.

The question now arises that if the normal displacement is a constant or, at most, a linear function of the spatial variable, y , (see equations 3.4 and 3.5), what meaning does it have to take the second derivative of

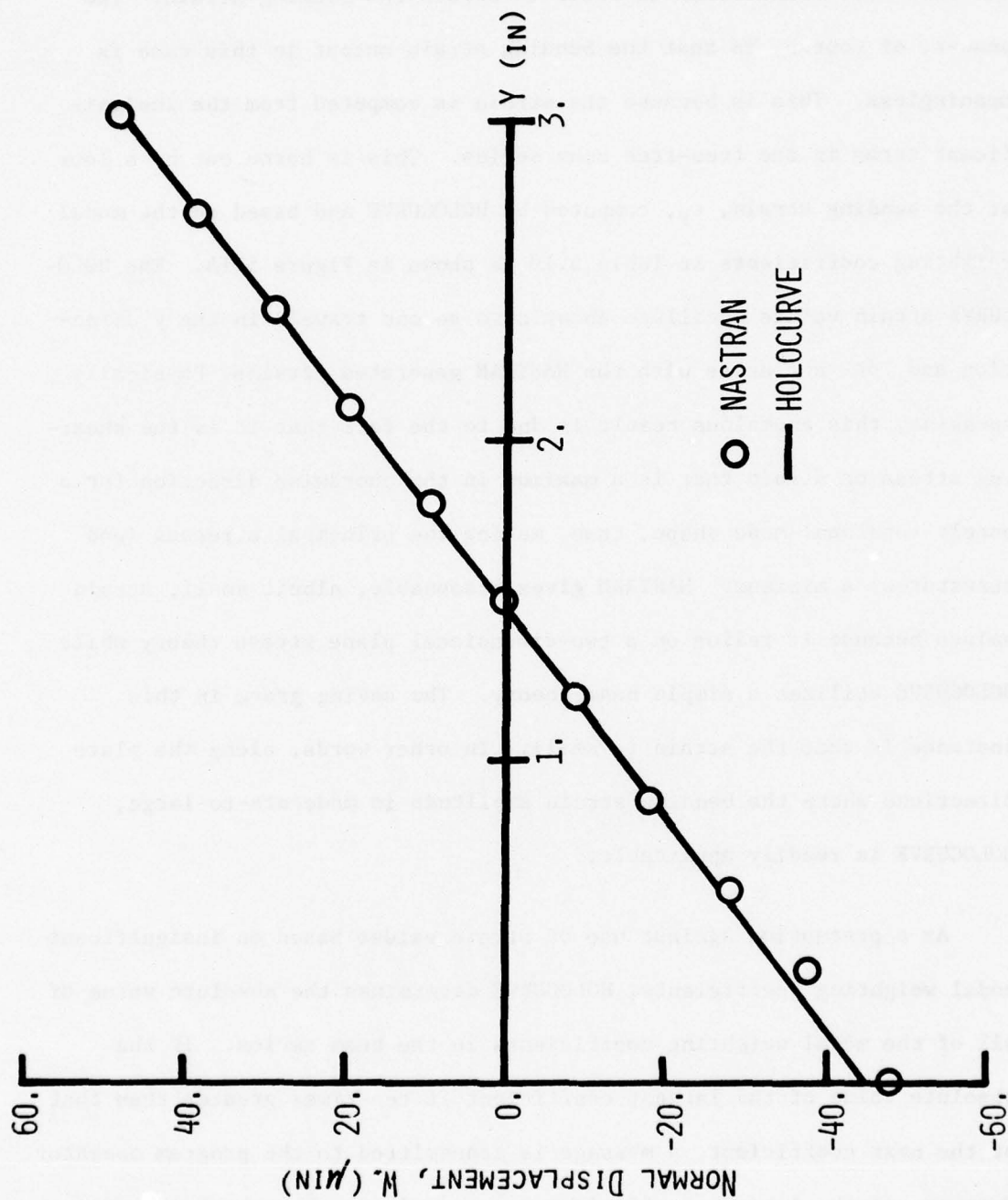


Figure 5.13 - Normal Displacement, W, vs. Chord, Y, at $X=1.0$ ", for Second Torsion Mode

the free-free beam series in order to obtain the bending strain? The answer, of course, is that the bending strain output in this case is meaningless. This is because the strain is computed from the insignificant terms in the free-free beam series. This is borne out by a look at the bending strain, ϵ_y , computed by HOLOCURVE and based on the modal weighting coefficients in Table 5.10 as shown in Figure 5.14. The HOLOCURVE strain values oscillate about zero as one travels in the y direction and do not agree with the NASTRAN generated strains. Physically speaking, this anomalous result is due to the fact that it is the shearing stress or strain that is a maximum in the chordwise direction for a purely torsional mode shape, thus, making the principal stresses (and curvatures) a minimum. NASTRAN gives reasonable, albeit small, strain values because it relies on a two-dimensional plane stress theory while HOLOCURVE utilizes a simple beam theory. The saving grace in this instance is that the strain is small. In other words, along the plate directions where the bending strain amplitude is moderate-to-large, HOLOCURVE is readily applicable.

As a precaution against use of strain values based on insignificant modal weighting coefficients, HOLOCURVE determines the absolute value of all of the modal weighting coefficients in the beam series. If the absolute value of the largest coefficient is ten times greater than that of the next coefficient, a message is transmitted to the program operator. Further, if the largest coefficient corresponds to the translational or rotational series component in the free-free beam series, a message to this effect is transmitted to the user.

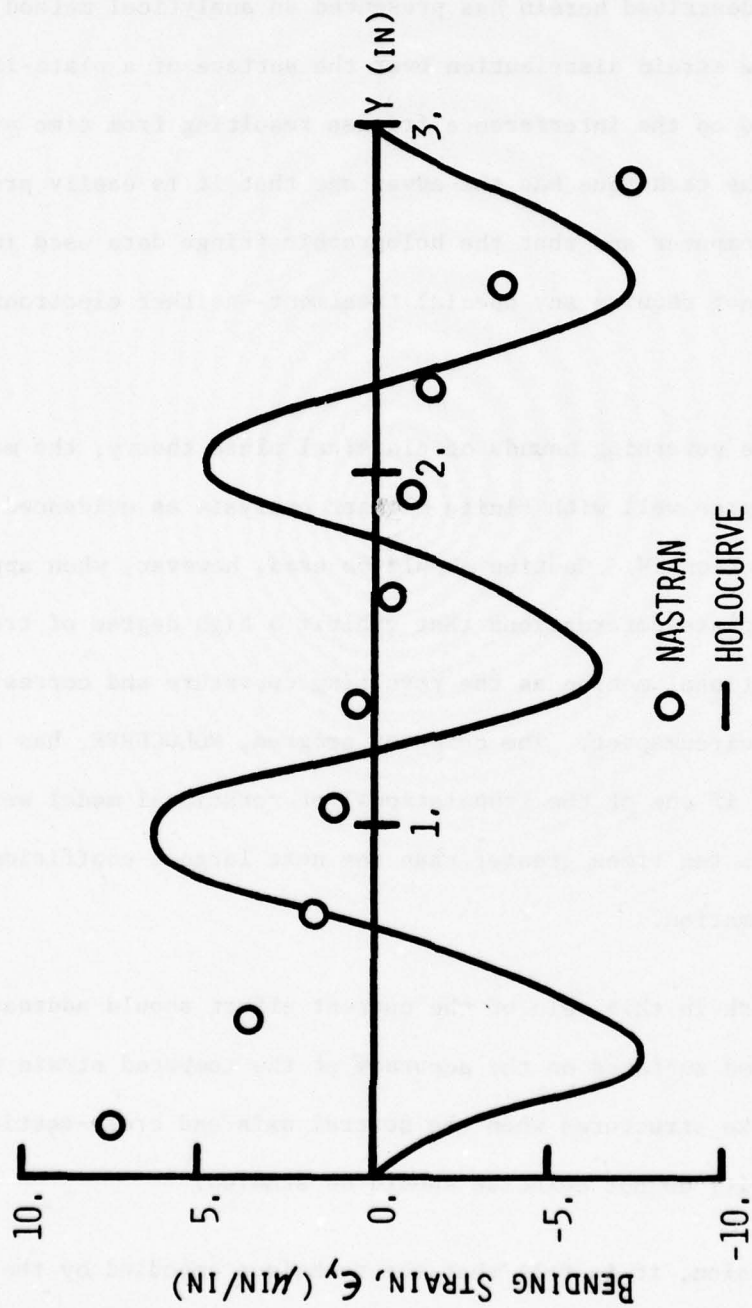


Figure 5.14 - Bending Strain, ϵ_y , vs. Chord, Y, at X=1.0" for Second Torsion Mode

SECTION VI

DISCUSSION AND CONCLUSION

The work described herein has presented an analytical method for determining the strain distribution over the surface of a plate-like structure based on the interference fringes resulting from time average holography. The technique has the advantage that it is easily programmed on a digital computer and that the holographic fringe data used in the solution does not require any special treatment--neither electronic nor optical.

Within the governing bounds of classical plate theory, the method was shown to agree well with finite element analysis as evidenced by the examples in Section IV. Caution should be used, however, when applying the method to plate deformations that exhibit a high degree of translational or rotational motion as the resulting curvature and corresponding strain may be circumspect. The computer program, HOLOCURVE, has a warning to this effect if one of the translational or rotational modal weighting coefficients is ten times greater than the next largest coefficient in the series approximation.

Future work in this vein of the current effort should address the effect of curved surfaces on the accuracy of the computed strain values. Also, plate-like structures when the neutral axis and cross-sectional center of gravity do not coincide should be studied.

In conclusion, it is felt that the technique embodied by the computer program, HOLOCURVE, will provide a useful tool for analyzing the surface strain distribution of vibration mode shapes of plate-like structures such as turbine engine blading.

APPENDIX A

PSEUDOINVERSE CALCULATION

$$A = \begin{bmatrix} 1 & 1 \\ 0 & 1 \\ 1 & 0 \end{bmatrix}$$

$$T = \begin{bmatrix} 1 & 0 & 1 \\ 0 & 1 & 0 \\ 0 & 0 & 1 \end{bmatrix} \quad T^{-1} = \begin{bmatrix} 1 & 0 & -1 \\ 0 & 1 & 0 \\ 0 & 0 & 1 \end{bmatrix}$$

$$A - A(A^T A)^{-1} A^T = \begin{bmatrix} 0 & 0 & 0 \\ 0 & 0 & 0 \\ 0 & 0 & 0 \end{bmatrix}$$

$$A^T A = \begin{bmatrix} 2 & 1 \\ 1 & 2 \end{bmatrix}$$

Given a $k \times p$ matrix, A , one can compute its pseudoinverse as follows:

1. Given:

$$A = \begin{bmatrix} 1 & 1 \\ 2 & 0 \\ 0 & 2 \end{bmatrix}, \quad k = 3, p = 2 \quad (\text{A-1})$$

2. We can then compute $A^T A$.

$$A^T A = \begin{bmatrix} 1 & 2 & 0 \\ 1 & 0 & 2 \end{bmatrix} \begin{bmatrix} 1 & 1 \\ 2 & 0 \\ 0 & 2 \end{bmatrix} = \begin{bmatrix} 5 & 1 \\ 1 & 5 \end{bmatrix} \quad (\text{A-2})$$

3. Compute the p non-negative square roots of the eigenvalues, s , of $A^T A$ to form the diagonal matrix, Σ .

$$\begin{vmatrix} 5-s & 1 \\ 1 & 5-s \end{vmatrix} = s^2 - 10s + 24 = 0 \quad (\text{A-3})$$

$$s_1 = 6, s_2 = 4$$

$$\Sigma = \begin{bmatrix} \sqrt{6} & 0 \\ 0 & 2 \end{bmatrix} \quad (\text{A-4})$$

4. Compute the orthonormalized eigenvectors, V_{iN} , of $A^T A$ to form the matrix V_N .

$$(A^T A - s_i I) V_i = 0, \quad i = 1, 2 \quad (A-5)$$

For $s_1 = 6$:

$$\left\{ \begin{bmatrix} 5 & 1 \\ 1 & 5 \end{bmatrix} - \begin{bmatrix} 6 & 0 \\ 0 & 6 \end{bmatrix} \right\} V_1 = 0 \quad (A-6)$$

$$\begin{bmatrix} -1 & 1 \\ 1 & -1 \end{bmatrix} \begin{pmatrix} x_1 \\ x_2 \end{pmatrix} = 0 \quad (A-7)$$

$$\text{Thus: } V_1 = \frac{\beta_1}{\sqrt{2}} \begin{pmatrix} 1 \\ 1 \end{pmatrix} \text{ and } V_{1N} = \frac{1}{\sqrt{2}} \begin{pmatrix} 1 \\ 1 \end{pmatrix} \quad (A-8)$$

Similarly, for $s_2 = 4$:

$$V_2 = \frac{\beta_2}{\sqrt{2}} \begin{pmatrix} 1 \\ -1 \end{pmatrix} \text{ and } V_{2N} = \frac{1}{\sqrt{2}} \begin{pmatrix} 1 \\ -1 \end{pmatrix} \quad (A-9)$$

Hence, from equations (A-8) and (A-9), we have:

$$V_N = \frac{1}{\sqrt{2}} \begin{bmatrix} 1 & 1 \\ 1 & -1 \end{bmatrix} = V_N^T \quad (A-10)$$

5. Compute the p orthonormalized eigenvectors, U_{1N} , based on the p largest eigenvalues of AA^T to form the matrix U .

$$AA^T = \begin{bmatrix} 1 & 1 \\ 2 & 0 \\ 0 & 2 \end{bmatrix} \begin{bmatrix} 1 & 2 & 0 \\ 1 & 0 & 2 \end{bmatrix} = \begin{bmatrix} 2 & 2 & 2 \\ 2 & 4 & 0 \\ 2 & 0 & 4 \end{bmatrix} \quad (A-11)$$

The eigenvalues of AA^T can be found to be:

$$s_1 = 6 \quad (A-12)$$

$$s_2 = 4$$

$$s_3 = 0$$

The two orthonormalized eigenvectors based on the largest two eigenvalues given in equation (A-12) can now be determined.

$$\text{For } s_1 = 6, \quad (A-13)$$

$$U_1 = \frac{\beta_1}{\sqrt{3}} \begin{pmatrix} 1 \\ 1 \\ 1 \end{pmatrix} \text{ and } U_{1N} = \frac{1}{\sqrt{3}} \begin{pmatrix} 1 \\ 1 \\ 1 \end{pmatrix}$$

$$\text{For } s_2 = 4,$$

$$U_2 = \frac{\beta_2}{\sqrt{2}} \begin{pmatrix} 0 \\ 1 \\ -1 \end{pmatrix} \text{ and } U_{2N} = \frac{1}{\sqrt{2}} \begin{pmatrix} 0 \\ 1 \\ -1 \end{pmatrix} \quad (A-14)$$

Hence,

$$U_N = \begin{bmatrix} \frac{1}{\sqrt{3}} & 0 \\ \frac{1}{\sqrt{3}} & \frac{1}{\sqrt{2}} \\ \frac{1}{\sqrt{3}} & -\frac{1}{\sqrt{2}} \end{bmatrix} \quad (A-15)$$

6. The matrix, A, can be represented as,

$$A = U_N \Sigma V_N^T \quad (A-16)$$

This can be checked by inserting equations
(A-15), (A-4), and (A-10) into (A-16) to get:

$$A = \begin{bmatrix} \frac{1}{\sqrt{3}} & 0 \\ \frac{1}{\sqrt{3}} & \frac{1}{\sqrt{2}} \\ \frac{1}{\sqrt{3}} & \frac{1}{\sqrt{2}} \end{bmatrix} \begin{bmatrix} \sqrt{6} & 0 \\ 0 & 2 \end{bmatrix} \begin{bmatrix} 1 & 1 \\ 1 & -1 \end{bmatrix}$$

$$= \begin{bmatrix} 1 & 0 \\ 1 & 1 \\ 1 & -1 \end{bmatrix} \begin{bmatrix} 1 & 1 \\ 1 & -1 \end{bmatrix}$$

$$= \begin{bmatrix} 1 & 1 \\ 2 & 0 \\ 2 & 2 \end{bmatrix} \quad \text{Q.E.D.} \quad (A-16)$$

7. The pseudoinverse of A is given as:

$$A^+ = V_N \Sigma^{-1} U_N^T$$

Hence:

$$A^+ = \frac{1}{\sqrt{2}} \begin{bmatrix} 1 & 1 \\ 1 & -1 \end{bmatrix} \begin{bmatrix} \frac{1}{\sqrt{6}} & 0 \\ 0 & \frac{1}{2} \end{bmatrix} \begin{bmatrix} \frac{1}{\sqrt{3}} & \frac{1}{\sqrt{3}} & \frac{1}{\sqrt{3}} \\ \frac{1}{\sqrt{2}} & -\frac{1}{\sqrt{2}} & 0 \end{bmatrix} \quad (\text{A-17})$$

$$A^+ = \frac{1}{12} \begin{bmatrix} 2 & 5 & -1 \\ 2 & -1 & 5 \end{bmatrix} \quad (\text{A-18})$$

It can be easily shown that equation (A-18) will satisfy the conditions for the pseudoinverse one of which is:

$$AA^+A = A \quad (\text{A-19})$$

APPENDIX B

HOLOCURVE LISTING

02/23/77 13.00.12

FTN 7,2+1+

PROGRAM TSL 74/14 OPT=1

```

-071 FORMAT(//X,*,HOW MANY *A2* 3EAM SERIES TEXIS WALL JL USED?----*)
  READ(7,*,02)TERMS
  N=TERMS
  IF(Q.EQ. 1) P=TERMS
  IF(P.EQ. 1) Q=TERMS
  WRITE(8,*,08)
  400 FORMAT(//X,*,INPUT NUMBER (F.P.) OF FRANGE VALUES.----*)
  READ(7,*,02) AFRG
  N=AFRG
  SEG=5HCHORD
  IF(Q.EQ. 1) SEG=5HSPAN
  WRITE(8,*,075) SEG
  4075 FORMAT(//X,*,INPUT *A5* LENGTH.----*)
  READ(7,*,02) ALGTH
  IF(P.EQ. 1) BL=ALGTH
  IF(Q.EQ. 1) AL=ALGTH
  IF(Q.EQ. 1) WRITE(8,*,10)
  409 FORMAT(//X,*,INPUT CONSTANT CHORD(Y) LOCATION.----*)
  410 FORMAT(//X,*,INPUT CONSTANT SPAN(X) LOCATION.----*)
  IF(Q.EQ. 1) READ(7,*,02) YCHORD
  IF(P.EQ. 1) READ(7,*,02) XSPAN
  DO 411 J=1,MQ
    IF(Q.EQ. 1) Y(J)=YCHORD
    411 IF(P.EQ. 1) X(J)=XSPAN
  C
  CALL NEWPAG
  WRITE(8,*,00)
  30 FORMAT(//X,*,WILL FRINGE OR DISPLACEMENT VALUES BE INPUT? TYPE "F"
    1 OR "O". ----*)
  READ(7,*,051) CVT
  001 FORMAT(A1)
  IF(Q.EQ. 1) WRITE(8,*,12)
  412 FORMAT(//X,*,INPUT PAIRS OF SPAN LOCATION,FRINGE VALUE DATA.*/
    1 *X,*,FREE FIELD FORMAT WITH EACH VALUE SEPARATED BY COMMAS.*/
    2//X,*,DATA=*)
  IF(P.EQ. 1) WRITE(8,*,13)
  413 FORMAT(//X,*,INPUT PAIRS OF CHORD LOCATION,FRINGE VALUE DATA.*/
    1 *X,*,FREE FIELD FORMAT WITH EACH VALUE SEPARATED BY COMMAS.*/
    2//X,*,DATA=*)
  IF(Q.EQ. 1) READ(7,*,*) (X(J),M(J),J=1,MJ)
  IF(P.EQ. 1) READ(7,*,*) (Y(J),W(J),J=1,MJ)
  ITHK=1
  IF(Q.EQ. 1) WRITE(8,*,0601)
  IF(P.EQ. 1) WRITE(8,*,0602)
  0601 FORMAT(//X,*,WILL DISTANCE FROM NEUTRAL AXIS VS. SPAN LOCATION BE
    1//X,*, INPUT - YES OR NO?----*)
  0602 FORMAT(//X,*,WILL DISTANCE FROM NEUTRAL AXIS VS. CHORD LOCATION BE
    1//X,*, INPUT - YES OR NO?----*)
  READ(7,*,051) ANS
  IF(ANS.EQ. 1) GO TO 530
  ITHK=2
  WRITE(8,*,062)
  062 FORMAT(//X,*,HOW MANY (SEGMENT LOCATION/NEUTRAL AXIS DISTANCE) */
    1 *X*VALUES WILL BE INPUT (MAX OF 20)?----*)
  READ(7,*,02) ATNK
  N.HK=ATNK

```

BEST AVAILABLE COPY


```

175      CALL NEWPAG
      3-AM=2HCF
      IF(P.EQ.1) BEAM=2HFF
      WRITE(6,9000) AMODE(L),L,BEAM
180      9000 FORMAT(5A,*,COMPUTATION COMPLETED FOR *A3,* MODE. DATA SET=*12,
      1/2X,*DO YOU WISH TO SEE MODAL WEIGHTING COEFFICIENTS FOR THE */
      25A,A2,* 3-AM SERIES - YES OR NO?---*)
      READ(7,9001) ANSWR
      9001 FORMAT(A3)
      IF(ANSWR.EQ.3HNO) GO TO 9003
      DO 9002 J=1,P
      9002 K=1,Q
      INC= K+A*(J-1)
      9002 WRITE(6,9004) J,K,AMN(INC)
      9004 FORMAT(6X,A(12,1X,12,*)= 1P12.5)
      9002 WRITE(6,9005)
      9005 FORMAT(//2X*WHERE A(P,1) = A(P) OR A(1,2) = B(1)*?)
      CALL LIMPJT(1)
      9003 CONTINUE
      C COMPUTE W(X,Y) FOR GIVEN VALUES OF X AND Y
      CALL NEWPAG
      9007 WRITE(6,9007) AMODE(L)
      9007 FORMAT(5X*DISPLACEMENT AND CURVATURE AS A FUNCTION OF*
      1/2X,*POSITION WILL NOW BE LISTED AND PLOTTED FOR MODE *A3/
      25A,*HOW MANY DATA POINTS DO YOU WANT (MAX OF 43)?----*)
      READ(7,9008) PTS
      9008 FORMAT(I5.5)
      C
      9009 IF(P.EQ.1) GO TO 9009
      AINC= AL/(PTS-1.)
      X0=-AINC
      GO TO 9011
      C
      9010 CONTINUE
      AINC=BL/(PTS-1.)
      Y0=-AINC
      C
      9011 IPTS=PTS
      DO 19 I=1,IPTS
      19 IF(P.EQ.1) Y0=Y0+AINC
      IF(Q.EQ.1) X0=X0+ALNC
      IF(Q.EQ.1) Y3=YC+Y0RD
      IF(P.EQ.1) X0=XSPAN
      CALL WDISP(X0,Y0,W3)
      CALL CURV(X0,Y0,AX2,WY2,I1HK,NIHK)
      C
      IF(P.EQ.1) XDATA(I)= Y0
      IF(Q.EQ.1) XDATA(I)=X0
      YTOR(1,1)=WD
      IF(Q.EQ.1) YSTOR(2,I)= WY2
      IF(P.EQ.1) YSTOR(3,I)= WY2
      13 CONTINUE
      C
      225      CALL NEWPAG
      C DISPLACEMENT AND CURVATURE OUTPUT*****
      DO 9016 L=1,2
      9016 L=L+1
      NUM=1

```

BEST AVAILABLE COPY

```

230      IF(ILL.EQ.2.AND.4.EQ.1) N04=2
      IF(ILL.EQ.2.AND.4.EQ.1) N04=3
      IF(ILL.EQ.1) WRITE(7,7050) AMODE(L)
7050    FORMAT(/X,'NORMAL DISPLACEMENT FOR MODE *40//')
      IF(ILL.EQ.2) WRITE(7,7051) AMODE(L)
7051    FORMAT(/X,'CURVATURE FOR MODE *49//')
      IF(ILL.EQ.2.AND.1THK.EQ.1) WRITE(7,7071)
7071    FORMAT(/X,'CURVAIJK BASED ON UNIT THICKNESS*//')
      IF(ILL.EQ.2.AND.1THK.EQ.2) WRITE(7,7072)
7072    FORMAT(/X,'CURVAIJK IS EQUIVALENT TO SIG-IN*//')
      WRITE(7,7015) OUTPUT(NUM)
7015    FORMAT(/X,'X*7X,Y*6X,A5,X*VONMILIZED *46//')
      DO 9016 I=1,IPTS
9016    YDATA(I)=YSTOR(NUM,I)
9015    CALL ENCKM(YDATA,YDATN,IPTS)
C
      IF(ILL.EQ.1) WRITE(7,7017)(XDATA(I),Y0,YDATA(I),YDAT(I),I=1,IPTS)
      IF(ILL.EQ.1) WRITE(7,7017)(X0,XDATA(I),YDATA(I),YDATN(I),I=1,IPTS)
9017    FORMAT(2X,0P,F0.3,2X,F6.3,2X,1PE12.5,0P,3X,F10.0)
      IF(ILL.EQ.1.AND.1TRIG.EQ.1) GO TO 1005
      IF(ILL.EQ.1.AND.1TRIG.EQ.1) GO TO 1001
      GO TO 1004
1001    IF(ILL.EQ.1) WRITE(7,1002) XMAG
      IF(ILL.EQ.1) WRITE(7,1003) XMAG
      IF(ILL.EQ.1) WRITE(7,1004) IFLAG,XMAG,IFLAG
1002    FORMAT(/X,'TRANSLATIONAL FF BEAM SERIES COMPONENT, B(1),*
1 /5X*IS* 1PE10.3,* TIMES THE NEXT LARGEST SERIES TERM.*//')
2 5X,*CURVATURE VALUES MUST BE VIEWED WITH CAUTION.*//')
1003    FORMAT(/X,'ROTATIONAL FF BEAM SERIES COMPONENT, B(2),*
1 /5X*IS* 1PE10.3,* TIMES THE NEXT LARGEST SERIES TERM.*//')
2 5X,*CURVATURE VALUES MUST BE VIEWED WITH CAUTION.*//')
1010    FORMAT(/X,'FF SERIES TERM, B(12),* IS* 1PE10.3,* TIMES*//')
1 2X,* THE NEXT LARGEST SERIES TERM INDICATING A STRONG*//')
2 5X,12,* FLEXURE COMPONENT.*//')
      GO TO 1004
1005    WRITE(7,1007) IFLAG,XMAG,IFLAG
1007    FORMAT(/X,'CF SERIES TERM, A(12),* IS* 1PE10.3,* TIMES*//')
1 5X,* THE NEXT LARGEST SERIES TERM INDICATING A STRONG*//')
2 5X,12,* FLEXURE COMPONENT.*//')
1004    CONTINUE
      CALL TIMEUT(I)
      CALL NEWFAG
C
      CALL PLIUT(IPTS,XDATA,YDATA,NUM,I,P,Q)
C
      CALL NEWFAG
      CONTINUE
9018    P=1.5 Q=1.5 PQ=1
      WRITE(7,7026)
7026    FORMAT(/X,'IS THERE MORE DATA TO BE ANALYZED (YES OR NO)?----')
9019    READ(7,527) ANS
527    FORMAT(A1)
      IF(ANS.EQ.1)N) STOP
      GO TO 403
      E 40

```

BEST AVAILABLE COPY

```

1      SUBROUTINE WDISP(X,Y,WD)
2
3      SUBROUTINE WDISP COMPUTES THE NORMAL DISPLACEMENT AT POINT (X,Y)
4      BASED ON THE SERIES EXPRESSION FOR W(X,Y).
5
6      I=INTEGER Z,P,Q
7      COMMON/ALZ/FX(20),FY(20),AMN(20),ALPH(20),BETA(20),P,Q,A,BL,
8      1 XMODEL
9
10     XMX,F,B,ALPHA)=
11     1+(1.+ALP+A)*EXP(-F*X/A)/2. -CJS(F*X/A)+ALPHA*SIN(F*X/A)
12     YMY,F,B,BETA)=
13     1+(1.+BET+A)*EXP(-F*Y/B)/2. +COS(F*Y/B) -3ETA*SIN(F*Y/B)
14
15     W)=0.
16     IF(P.EQ.1) GO TO 642
17     JU 137 J=1,P
18     PHI =XM(X,FX(J),AL,ALPH(J))
19     GU TO 10
20
21     137 WJ=WD+AMN(J)*PHI
22     GU TO 10
23
24     042 DO 136 K=1,Q
25     IF(K.GT.2) GO TO 130
26     GU TO (131,132),K
27     130 PHI =YV(Y,FY(K),BL,BETA(K))
28     GU TO 136
29     131 PHI=1.
30     GO TO 135
31     132 PHI= SQRT(3.)*(1.-2.*Y/BL)
32     133 WJ= WJ+AMN(K)*PHI
33     13 CONTINUE
34     RETURN
35     END

```

BEST AVAILABLE COPY

1 SUBROUTINE CURV(X,Y,EX,EY,I1HK,NTHK)
COMMON/THICK/X1HK(20),Y1HK(20)
DIMENSION TEMP(6)

3 INTEGER P,Q,PQ
COMMON/AZ/FX(20),FY(20),AN(O),ALPH(20),BETA(20),P,Q,AL,DL,
1 XMODE

10 X1(X,F,A,ALPHA)= (1.-ALPHA)*EXP(F*X/A)/2.
1 + (1.-ALPHA)*EXP(-F*X/A)/2. -COS(F*X/A) + ALPHA*SIN(F*X/A)
X1(X,F,A,-ALPHA)=(F/A) * ((1.-ALPHA)*EXP(F*X/A)/2.
1 - (1.-ALPHA)*EXP(-F*X/A)/2. + SIN(F*X/A) + ALPHA*COS(F*X/A))
X2(X,F,A,-ALPHA)=(F/A)*2*((1.-ALPHA)*EXP(F*X/A)/2.
1 + (1.-ALPHA)*EXP(-F*X/A)/2. +COS(F*X/A) -ALPHA*SIN(F*X/A))

15 Y1(Y,F,B,BETA)= (1.-BETA)*EXP(F*Y/B)/2.
1 + (1.-BETA)*EXP(-F*Y/B)/2. +COS(F*Y/B) -BETA*SIN(F*Y/B)
Y1(Y,F,B,BETA)=(F/B) * ((1.-BETA)*EXP(F*Y/B)/2.
1 - (1.-BETA)*EXP(-F*Y/B)/2. -SIN(F*Y/B) -BETA*COS(F*Y/B))
Y2(Y,F,B,BETA)=(F/B)*2*((1.-BETA)*EXP(F*Y/B)/2.
1 + (1.-BETA)*EXP(-F*Y/B)/2. -COS(F*Y/B) +BETA*SIN(F*Y/B))

25 C COMPUTE STRAINS

EX=0.

EY=0.

IF(P.EQ. 1) GO TO 642

GO 137 J=1,P

PEX= X2(X,FX(J),AL,ALPH(J))

137 EX=EX+AMN(J)*PEX

GO TO 10

642 DO 138 K=1,Q

IF(K.GT. 2) GO TO 130

GO TO (131,132),K

130 PEY=Y2(Y,FY(K),BL,BETA(K))

GO TO 136

131 PEY=0.

GO TO 138

132 PEY=0.

135 EY=EY+AMN(K)*PEY

10 Z=1.

IF(I1HK.EQ. 1) GO TO 50

IF(P.EQ. 1 .AND. I1HK.EQ. 2) CALL INTERP(X1HK,Y1HK,NTHK,2,Y,Z,

1 TEMP,IER)

IF(Q.EQ.1.AND.I1HK.EQ.2) CALL INTERP(X1HK,Y1HK,NTHK,2,X,Z,

1 TEMP,IER)

IF(P.EQ. 1) EY= Z/2.*EY

IF(Q.EQ. 1) EX= Z/2.*EX

50 RETURN

END

0041+0

00360
003370
0020
003400
003410
003420
003430
003440
003450
003460
003470
003480
003490
003500
003510
003520
003530
003540
003550
003560
003570
003600
003610

BEST AVAILABLE COPY


```

1  SUBROUTINE FREQ
   COMMON/FAZ/FX(20),FY(20),AMN(6),ALPH(20),DELTA(20),P,Q,AL,BL,
   1  XMODE
   C DEFINE COSH AND SINH FUNCTIONS
   COSH(X) = (EXP(X)+EXP(-X))/2.
   SINH(X) = (EXP(X)-EXP(-X))/2.
   C CHARACTERISTIC EQS. AND THEIR DERIVATIVES
   FFX(X) = COS(X)*COSH(X) - 1.
   FY(X) = -SIN(X)*COSH(X) + COS(X)*SINH(X)
   GX(X) = COS(X)*COSH(X) + 1.
   GY(X) = FP(X)
   C FIXED-FREE BEAM FREQUENCIES
   DATA (FX(I),I=1,6)/ 1.8751041, 4.0940911, 7.867514,
   1  10.9952407, 14.1371664, 17.276753 /
   C FREE-FREE BEAM FREQUENCIES
   DATA (FY(I),I=3,6)/ 1.7300406, 7.0032040, 11.1996019, 14.1971655 /
   DO 299 I=7,20
   PI= 3.14159265
   AI=1
   FX(I) = (2.*AI-1.)*PI/2.
   299 FY(I) = (2.*AI-3.)*PI/2.
   EXOR= 1.E-12
   DO 25 I=1,20
   RM= FX(I)
   C
   27 RM1= RM - CC(RM)/CP(RM)
   IF( ABS(RM1-RM) .LT. ERROR) GO TO 28
   RM= RM1
   GO TO 27
   C
   28 FX(I)= RM
   ALPH(I)= (COS(RM)+COSH(RM))/(SIN(RM)+SINH(RM))
   IF( I .LE. 2) GO TO 26
   RM= FY(I)
   29 RM1= RM - FF(RM)/FP(RM)
   IF( ABS(RM1-RM) .LT. ERROR) GO TO 30
   RM= RM1
   GO TO 29
   C
   30 FY(I)= RM
   DELTA(I)= (COS(RM) - COSH(RM))/(SIN(RM) - SINH(RM))
   25 CONTINUE
   RETURN
   END

```

BEST AVAILABLE COPY

```

1  SUBROUTINE PLIDAT(IPIS,XDATA,YDATA,NUM,P,2)
   DIMENSION IM(14),IXXX(13),IMYY(13),IX(3),IY(3)
   DIMENSION XDATA(IPIS),YDATA(IPIS)
   INTEGER P,2
3  DATA IM/07,32,00,73,03,00,70,03,07,09,7,03,70,04/
   DATA IMXX/07,00,00,32,07,05,32,00,05,04,05,32,09/
   DATA IMYY/07,03,03,32,07,05,32,00,05,04,05,32,03/
10  DATA IX/00,32,00,03,00,63,70,11/
   DATA IY/00,32,00,07,72,79,62,03,11/
   CALL INITI(30)
   CALL FINITI
   CALL NPTS(IPIS)
   CALL CHECK(XDATA,YDATA)
   CALL SYMBL(1)
   CALL USPL-Y(XDATA,YDATA)
   CALL MOVABS(500,32)
   IF(P.EQ. 1) CALL LABEL(9,IY)
   IF(Q.EQ. 1) CALL LABEL(9,IX)
20  CALL MOVABS(48,030)
   IF(NUM.EQ. 1) CALL LABEL(14,14)
   IF(NUM.EQ. 2) CALL LABEL(13,IMXX)
   IF(NUM.EQ. 3) CALL LABEL(13,IMYY)
   CALL INPUT(I)
   CALL FINITI(0,700)
   RETURN
   END
30

```

BEST AVAILABLE COPY

SUBROUTINE CONVKT 74/4 UFT=1

```

1  SUBROUTINE CONVKT(M,N)
   DIMENSION W(N),BES0(39)
   BES0(1)=2.0482555
   PI=3.14159265
   DO 11 I=2,39
     A=4.*FLOAT(I)-1.
     P=PI*A
10  BES0(I)= .25*P*(1.+2./P**2- 02./3./P**4
      1 +15110./15./P**6 - 1255474./105./P**8
      2 +836882-292./315./P**10)
     XLAM=C320.E-0/2.939
     DO 11 I=1,N
       K=1FIX(ABS(W(I)))
       IF(K .EQ. 0) GO TO 11
       SUN=1.
       IF(W(I) .LT. 0.) SGN=-1.
       W(I)=SGN*XLAM*BES0(K)/(4.*PI)
11  IF(W(I) .EQ. 0.) W(I)=0.
     RETURN
   END

```

000010
 000020
 000025
 000030
 000040
 000050
 000060
 000070
 000080
 000090
 000100
 000110
 000120
 000125
 000130
 000140
 000150
 000160
 000170
 000180

BEST AVAILABLE COPY

```

1  SUBROUTINE COMPAN(IFLAG1,XMAG,TRIG)
2  C THIS SUB-ROUTINE COMPARES THE BEAM SERIES TERMS WITH EACH OTHER TO SEE IF
3  C ONE TERM IS APPRECIABLY LARGER THAN THE OTHERS. THIS IS PARTICULARLY
4  C IMPORTANT FOR THE CASE OF THE FREE-FREE BEAM SERIES WHERE THE
5  C TRANSLATIONAL OR ROTATIONAL MODES CAN DOMINATE GIVING RISE TO
6  C ERRONEOUS SECOND DERIVATIVES.
7  C
8  C
9  C
10 C
11 C
12 C
13 C
14 C
15 C
16 C
17 C
18 C
19 C
20 C
21 C
22 C
23 C
24 C
25 C
26 C
27 C
28 C
29 C
30 C
31 C
32 C
33 C
34 C
35 C
36 C
37 C
38 C
39 C
40 C
41 C
42 C
43 C
44 C
45 C
46 C
47 C
48 C
49 C
50 C
51 C
52 C
53 C
54 C
55 C
56 C
57 C
58 C
59 C
60 C
61 C
62 C
63 C
64 C
65 C
66 C
67 C
68 C
69 C
70 C
71 C
72 C
73 C
74 C
75 C
76 C
77 C
78 C
79 C
80 C
81 C
82 C
83 C
84 C
85 C
86 C
87 C
88 C
89 C
90 C
91 C
92 C
93 C
94 C
95 C
96 C
97 C
98 C
99 C
100 C
101 C
102 C
103 C
104 C
105 C
106 C
107 C
108 C
109 C
110 C
111 C
112 C
113 C
114 C
115 C
116 C
117 C
118 C
119 C
120 C
121 C
122 C
123 C
124 C
125 C
126 C
127 C
128 C
129 C
130 C
131 C
132 C
133 C
134 C
135 C
136 C
137 C
138 C
139 C
140 C
141 C
142 C
143 C
144 C
145 C
146 C
147 C
148 C
149 C
150 C
151 C
152 C
153 C
154 C
155 C
156 C
157 C
158 C
159 C
160 C
161 C
162 C
163 C
164 C
165 C
166 C
167 C
168 C
169 C
170 C
171 C
172 C
173 C
174 C
175 C
176 C
177 C
178 C
179 C
180 C
181 C
182 C
183 C
184 C
185 C
186 C
187 C
188 C
189 C
190 C
191 C
192 C
193 C
194 C
195 C
196 C
197 C
198 C
199 C
200 C
201 C
202 C
203 C
204 C
205 C
206 C
207 C
208 C
209 C
210 C
211 C
212 C
213 C
214 C
215 C
216 C
217 C
218 C
219 C
220 C
221 C
222 C
223 C
224 C
225 C
226 C
227 C
228 C
229 C
230 C
231 C
232 C
233 C
234 C
235 C
236 C
237 C
238 C
239 C
240 C
241 C
242 C
243 C
244 C
245 C
246 C
247 C
248 C
249 C
250 C
251 C
252 C
253 C
254 C
255 C
256 C
257 C
258 C
259 C
260 C
261 C
262 C
263 C
264 C
265 C
266 C
267 C
268 C
269 C
270 C
271 C
272 C
273 C
274 C
275 C
276 C
277 C
278 C
279 C
280 C
281 C
282 C
283 C
284 C
285 C
286 C
287 C
288 C
289 C
290 C
291 C
292 C
293 C
294 C
295 C
296 C
297 C
298 C
299 C
300 C
301 C
302 C
303 C
304 C
305 C
306 C
307 C
308 C
309 C
310 C
311 C
312 C
313 C
314 C
315 C
316 C
317 C
318 C
319 C
320 C
321 C
322 C
323 C
324 C
325 C
326 C
327 C
328 C
329 C
330 C
331 C
332 C
333 C
334 C
335 C
336 C
337 C
338 C
339 C
340 C
341 C
342 C
343 C
344 C
345 C
346 C
347 C
348 C
349 C
350 C
351 C
352 C
353 C
354 C
355 C
356 C
357 C
358 C
359 C
360 C
361 C
362 C
363 C
364 C
365 C
366 C
367 C
368 C
369 C
370 C
371 C
372 C
373 C
374 C
375 C
376 C
377 C
378 C
379 C
380 C
381 C
382 C
383 C
384 C
385 C
386 C
387 C
388 C
389 C
390 C
391 C
392 C
393 C
394 C
395 C
396 C
397 C
398 C
399 C
400 C
401 C
402 C
403 C
404 C
405 C
406 C
407 C
408 C
409 C
410 C
411 C
412 C
413 C
414 C
415 C
416 C
417 C
418 C
419 C
420 C
421 C
422 C
423 C
424 C
425 C
426 C
427 C
428 C
429 C
430 C
431 C
432 C
433 C
434 C
435 C
436 C
437 C
438 C
439 C
440 C
441 C
442 C
443 C
444 C
445 C
446 C
447 C
448 C
449 C
450 C
451 C
452 C
453 C
454 C
455 C
456 C
457 C
458 C
459 C
460 C
461 C
462 C
463 C
464 C
465 C
466 C
467 C
468 C
469 C
470 C
471 C
472 C
473 C
474 C
475 C
476 C
477 C
478 C
479 C
480 C
481 C
482 C
483 C
484 C
485 C
486 C
487 C
488 C
489 C
490 C
491 C
492 C
493 C
494 C
495 C
496 C
497 C
498 C
499 C
500 C
501 C
502 C
503 C
504 C
505 C
506 C
507 C
508 C
509 C
510 C
511 C
512 C
513 C
514 C
515 C
516 C
517 C
518 C
519 C
520 C
521 C
522 C
523 C
524 C
525 C
526 C
527 C
528 C
529 C
530 C
531 C
532 C
533 C
534 C
535 C
536 C
537 C
538 C
539 C
540 C
541 C
542 C
543 C
544 C
545 C
546 C
547 C
548 C
549 C
550 C
551 C
552 C
553 C
554 C
555 C
556 C
557 C
558 C
559 C
560 C
561 C
562 C
563 C
564 C
565 C
566 C
567 C
568 C
569 C
570 C
571 C
572 C
573 C
574 C
575 C
576 C
577 C
578 C
579 C
580 C
581 C
582 C
583 C
584 C
585 C
586 C
587 C
588 C
589 C
590 C
591 C
592 C
593 C
594 C
595 C
596 C
597 C
598 C
599 C
600 C
601 C
602 C
603 C
604 C
605 C
606 C
607 C
608 C
609 C
610 C
611 C
612 C
613 C
614 C
615 C
616 C
617 C
618 C
619 C
620 C
621 C
622 C
623 C
624 C
625 C
626 C
627 C
628 C
629 C
630 C
631 C
632 C
633 C
634 C
635 C
636 C
637 C
638 C
639 C
640 C
641 C
642 C
643 C
644 C
645 C
646 C
647 C
648 C
649 C
650 C
651 C
652 C
653 C
654 C
655 C
656 C
657 C
658 C
659 C
660 C
661 C
662 C
663 C
664 C
665 C
666 C
667 C
668 C
669 C
670 C
671 C
672 C
673 C
674 C
675 C
676 C
677 C
678 C
679 C
680 C
681 C
682 C
683 C
684 C
685 C
686 C
687 C
688 C
689 C
690 C
691 C
692 C
693 C
694 C
695 C
696 C
697 C
698 C
699 C
700 C
701 C
702 C
703 C
704 C
705 C
706 C
707 C
708 C
709 C
710 C
711 C
712 C
713 C
714 C
715 C
716 C
717 C
718 C
719 C
720 C
721 C
722 C
723 C
724 C
725 C
726 C
727 C
728 C
729 C
730 C
731 C
732 C
733 C
734 C
735 C
736 C
737 C
738 C
739 C
740 C
741 C
742 C
743 C
744 C
745 C
746 C
747 C
748 C
749 C
750 C
751 C
752 C
753 C
754 C
755 C
756 C
757 C
758 C
759 C
760 C
761 C
762 C
763 C
764 C
765 C
766 C
767 C
768 C
769 C
770 C
771 C
772 C
773 C
774 C
775 C
776 C
777 C
778 C
779 C
780 C
781 C
782 C
783 C
784 C
785 C
786 C
787 C
788 C
789 C
790 C
791 C
792 C
793 C
794 C
795 C
796 C
797 C
798 C
799 C
800 C
801 C
802 C
803 C
804 C
805 C
806 C
807 C
808 C
809 C
810 C
811 C
812 C
813 C
814 C
815 C
816 C
817 C
818 C
819 C
820 C
821 C
822 C
823 C
824 C
825 C
826 C
827 C
828 C
829 C
830 C
831 C
832 C
833 C
834 C
835 C
836 C
837 C
838 C
839 C
840 C
841 C
842 C
843 C
844 C
845 C
846 C
847 C
848 C
849 C
850 C
851 C
852 C
853 C
854 C
855 C
856 C
857 C
858 C
859 C
860 C
861 C
862 C
863 C
864 C
865 C
866 C
867 C
868 C
869 C
870 C
871 C
872 C
873 C
874 C
875 C
876 C
877 C
878 C
879 C
880 C
881 C
882 C
883 C
884 C
885 C
886 C
887 C
888 C
889 C
890 C
891 C
892 C
893 C
894 C
895 C
896 C
897 C
898 C
899 C
900 C
901 C
902 C
903 C
904 C
905 C
906 C
907 C
908 C
909 C
910 C
911 C
912 C
913 C
914 C
915 C
916 C
917 C
918 C
919 C
920 C
921 C
922 C
923 C
924 C
925 C
926 C
927 C
928 C
929 C
930 C
931 C
932 C
933 C
934 C
935 C
936 C
937 C
938 C
939 C
940 C
941 C
942 C
943 C
944 C
945 C
946 C
947 C
948 C
949 C
950 C
951 C
952 C
953 C
954 C
955 C
956 C
957 C
958 C
959 C
960 C
961 C
962 C
963 C
964 C
965 C
966 C
967 C
968 C
969 C
970 C
971 C
972 C
973 C
974 C
975 C
976 C
977 C
978 C
979 C
980 C
981 C
982 C
983 C
984 C
985 C
986 C
987 C
988 C
989 C
990 C
991 C
992 C
993 C
994 C
995 C
996 C
997 C
998 C
999 C
1000 C

```

BEST AVAILABLE COPY

SUBROUTINE UNOUM 7474 JPT=1

```

1      SUBROUTINE UNOUM(YD,YN,IPTS)
2      DIMENSION YL(-3),YN(+3)
3      C FIND LARGEST YD VALUE
4      BIG=0.
5      DO 10 I=1,IPTS
6      10 IF(A35(YD(I)) .GT. BIG) BIG=A35(YD(I))
7      C NORMALIZE YD DATA
8      DO 11 I=1,IPTS
9      11 YN(I)= YD(I)/BIG
10     RETURN
11     END

```

BEST AVAILABLE COPY

USA NJ3/3E L41-H 6000 JMR1 03/29/77
 13.55.09.J40A3M FROM /4E
 13.55.09.1P J0002752 WORKJ - FILE INPUT , OC 00
 13.55.09.1P J101012,C1010300,S1051.P720030 YACB
 13.55.09.1P J101012,C1010300,S1051.P720030 YACB
 13.55.12.FT 1.
 13.55.36.L0CKIN.
 13.59.42. 3.673 CP SECONDS COMPILE:ION TIME
 13.59.42.ATTACH,C00000,LU=4054321,N=ASD.
 13.59.42.PFN IS
 13.59.42.C00000
 13.59.42.PF CYCLE NU. = 001
 13.59.42.ATTACH,TEKL13,TEK,RONIXL13,LO=P7200612.
 13.59.43.PF CYCLE NU. = 999
 13.59.43.ATTACH,IMSL,IMSL,IO=X604321,SN=ASD.
 13.59.43.PF CYCLE NU. = 001
 13.59.43.LIBRARY,TEKL13,IMSL.
 13.59.43.XEQUEST,ABS,PF.
 13.59.40.443,PAR.
 13.59.46.L0SET,LIB=C00000.
 13.59.47.L04J,L00.
 13.59.47.N000,ABS.
 14.00.07.PURGE,LF1,NEW,CY=1.
 14.00.08.PA 10= P720030 PFN=NEW
 14.00.08.PR CY= 001 00023008 MORUS.
 14.00.08.CATALOG,ABS,NEW,CY=1,KP=50.
 14.00.08.INITIAL CAT4LUG
 14.00.09.CT 10= P720030 PFN=NEW
 14.00.09.UT CY= 001 00023008 MORUS.
 14.00.09.OP J0008768 MORUS - FILE OUTPUT , 03 40
 14.00.09.15 40592 MORUS (40592 MAX USED)
 14.00.09.S24 7*000 MORUS MAXIMUM
 14.00.09.0PA 6.592 SEC. 2.905 ADJ.
 14.00.09.10 9.500 SEC. 4.752 ADJ.
 14.00.09.04 303.437 KMS. 2.947 ADJ.
 14.00.09.00JUS 10.630
 14.00.09.003T .63
 14.00.09.00 PP 30.610 SEC. DATE 03/23/77
 14.00.09.EJ END OF JOB, AE P720030.

***** JMDA3M /// END OF LIST ////

BEST AVAILABLE COPY

APPENDIX C

HOLOCURVE EXAMPLE

ASD COMPUTER CENTER INTERCOM 4.5
SYSTEM CSA

DATE 06/01/77 TIME 10.50.12.

PLEASE LOGIN

LOGIN,P720611,88,305

06/01/77 LOGGED IN AT 10.50.35.
WITH USER-ID JR

EQUIP/PORT 16/031

COMMAND- ATTACH,HOLD,NEW,CY=1, ID=P720630

COMMAND- HOLD

<<<< PROGRAM HOLOCLURE - VERSION 23 MAY 77 1800 >>>>

ANSWER ALL QUESTIONS IN FLOATING POINT OR
ALPHANERICALLY AS INDICATED

DATA SET NUMBER 1

WHAT IS THE MODE NAME (8H)?---2 FLEX

WILL OUTPUT BE BASED ON CLAMPED-FREE (CF) OR
FREE-FREE (FF) BEAM SERIES? TYPE CF OR FF.---CF

HOW MANY CF BEAM SERIES TERMS WILL BE USED?---5.

INPUT NUMBER (F.P.) OF FRINGE VALUES.---7.

INPUT SPAN LENGTH.---7.

INPUT CONSTANT CHORD(Y) LOCATION.---.5

WILL FRINGE OR DISPLACEMENT VALUES BE INPUT? TYPE "F" OR "D". ---F

INPUT PAIRS OF SPAN LOCATION,FRINGE VALUE DATA.
FREE FIELD FORMAT WITH EACH VALUE SEPARATED BY COMMAS.

DATA=1.,-5.,2.,-11.,3.,-12.,4.,-8.,4.94,0.,6.,9.,7.,16.

WILL DISTANCE FROM NEUTRAL AXIS US. SPAN LOCATION BE
INPUT - YES OR NO?---NO

DO YOU WISH TO SEE INPUT DATA (YES OR NO)?... YES

2 FLEX MODE FRINGE VALUES FOR (P,Q) =5, 1

I= 1	X, Y= 1.0000	.5000	F= -5.00
I= 2	X, Y= 2.0000	.5000	F= -11.00
I= 3	X, Y= 3.0000	.5000	F= -12.00
I= 4	X, Y= 4.0000	.5000	F= -8.00
I= 5	X, Y= 4.9400	.5000	F= 0.00
I= 6	X, Y= 6.0000	.5000	F= 9.00
I= 7	X, Y= 7.0000	.5000	F= 16.00

COMPUTATION COMPLETED FOR 2 FLEX MODE. DATA SET= 1
DO YOU WISH TO SEE MODAL WEIGHTING COEFFICIENTS FOR THE
CF BEAM SERIES - YES OR NO?---YES

AK 1 1) = 1.17223E-05

AK 2 1) = -5.00400E-05

AK 3 1) = -1.25548E-05

AK 4 1) = -4.61346E-07

AK 5 1) = -1.49835E-06

WHERE AK(P,1) = AK(P) OR AK(1,Q) = BK(Q)

NON-UNIFORM, DYNAMIC BEHAVIOR DO NOT PRESENT (MAY BE 10% TO 12%
VARIATION IN THE FIRST MODE) BUT THE FOLLOWING ARE MORE 5 AFTER
DISCRETELY AND CONSIDERABLE AS A FUNCTION OF

DISPLACEMENT AND CURVATURE AS A FUNCTION OF
 POSITION WILL NOW BE LISTED AND PLOTTED FOR MODE 2 FLEX
 HOW MANY DATA POINTS DO YOU WANT (MAX OF 40)?---15.

HERE WE GO - 15.0 OF 15.0 = 100%

1 1 1 1 1 1 1 1 1 1 1 1 1 1 1

2 2 2 2 2 2 2 2 2 2 2 2 2 2 2

3 3 3 3 3 3 3 3 3 3 3 3 3 3 3

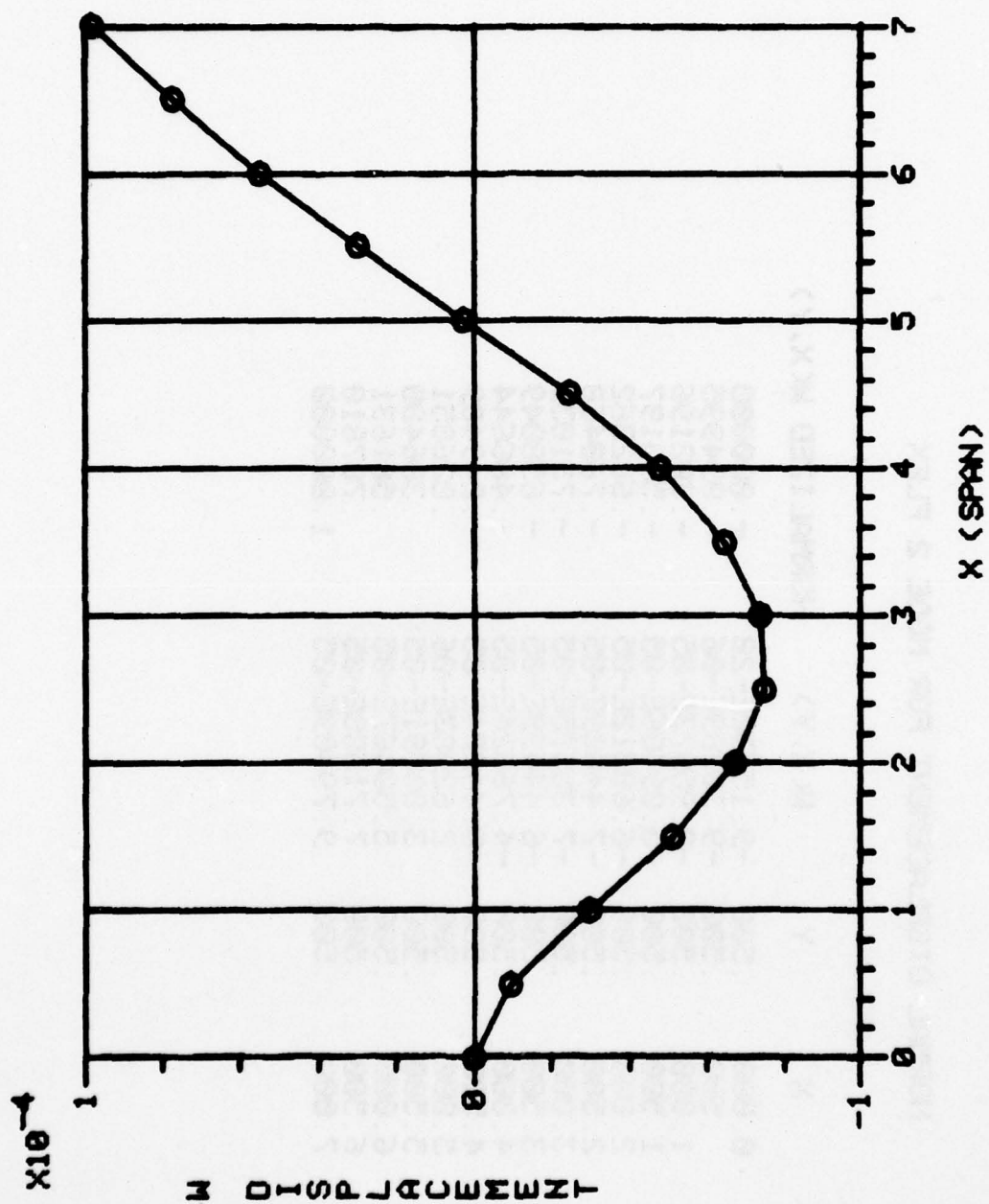
4 4 4 4 4 4 4 4 4 4 4 4 4 4 4

5 5 5 5 5 5 5 5 5 5 5 5 5 5 5

OK NEW SERIES - ALL OK MODE 2 FLEX
 DO YOU WISH TO GET MORE DETAILS OF COEFFICIENTS FOR THE
 CURVATURE CORRELATION FOR 5 FLEX MODE ONLY YES/NO

NORMAL DISPLACEMENT FOR MODE 2 FLEX

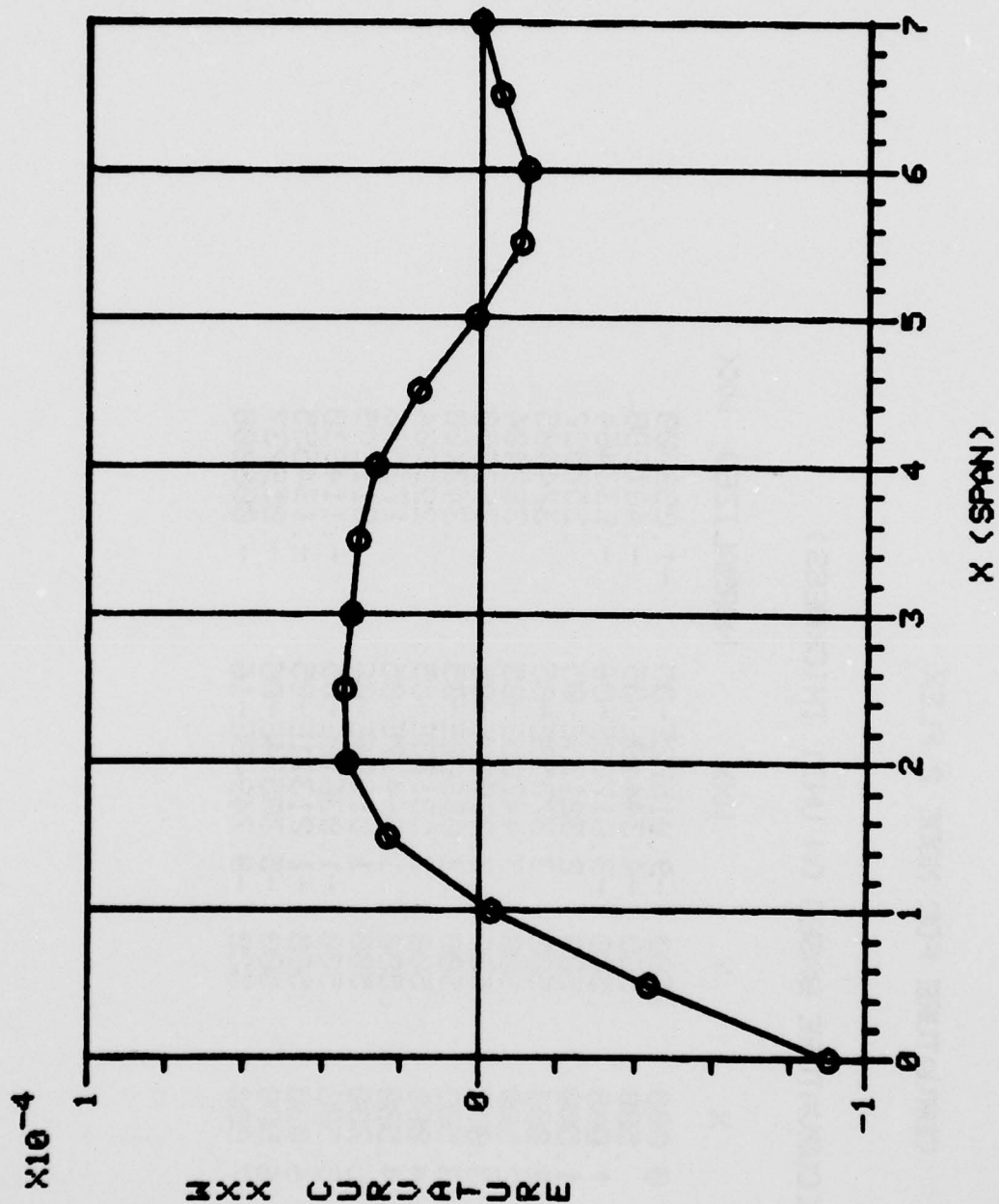
X	Y	WKX,Y>	NORMALIZED WKX,Y>
0.000	.500	-9.15730E-20	-.000000
.500	.500	-9.30389E-06	-.094995
1.000	.500	-2.95973E-05	-.302196
1.500	.500	-5.09486E-05	-.520197
2.000	.500	-6.68312E-05	-.682362
2.500	.500	-7.44809E-05	-.760468
3.000	.500	-7.35575E-05	-.751039
3.500	.500	-6.44499E-05	-.658049
4.000	.500	-4.76624E-05	-.486644
4.500	.500	-2.44274E-05	-.249409
5.000	.500	2.62983E-06	.026851
5.500	.500	3.00091E-05	.306400
6.000	.500	5.50067E-05	.561631
6.500	.500	7.71588E-05	.787810
7.000	.500	9.79409E-05	1.000000



CURVATURE FOR MODE 2 FLEX

< CURVATURE BASED ON UNIT THICKNESS >

X	Y	WXX	NORMALIZED WXX
0.000	.500	-9.01572E-05	-1.000000
.500	.500	-4.34449E-05	-.481880
1.000	.500	-3.01700E-06	-.033464
1.500	.500	2.32179E-05	.257527
2.000	.500	3.37553E-05	.374405
2.500	.500	3.44765E-05	.382404
3.000	.500	3.27090E-05	.362800
3.500	.500	3.09600E-05	.343400
4.000	.500	2.63173E-05	.291904
4.500	.500	1.56437E-05	.173516
5.000	.500	1.01384E-06	.011245
5.500	.500	-1.03618E-05	-.114930
6.000	.500	-1.21311E-05	-.134555
6.500	.500	-5.38574E-06	-.059737
7.000	.500	-9.74940E-16	-.000000



IS THERE MORE DATA TO BE ANALYZED (YES OR NO)?---NO

STOP

.436 CP SECONDS EXECUTION TIME
COMMAND- LOGOUT

CPA 2.771 SEC. 1.202 ADJ.

CRUS 2.676

CONNECT TIME 0 HRS. 14 MIN.
06/01/77 LOGGED OUT AT 11.04.06.

APPENDIX D

LLSQAR DESCRIPTION

AD-A046 153

AIR FORCE AERO PROPULSION LAB WRIGHT-PATTERSON AFB OHIO F/G 20/11
QUANTITATIVE DISPLACEMENT AND STRAIN DISTRIBUTION OF VIBRATING --ETC(U)
JUL 77 J C MACBAIN

UNCLASSIFIED

AFAPL-TR-77-44

NL

2 of 2
ADA046153



END
DATE
FILMED
12-77
DDC

```

SUBROUTINE LLSQAR (A,B,M,NA,NB,IA,IB,IDGT,WKAREA,IER)
C-----S-----LIBRARY 3-----
C
C  FUNCTION          - LEAST SQUARES SOLUTION OF OVERDETERMINED
C                    - SYSTEM OF LINEAR EQUATIONS
C  USAGE            - CALL LLSQAR(A,B,M,NA,NB,IA,IB,IDGT,WKAREA,IER)
C  PARAMETERS      A  - THE COEFFICIENT MATRIX OF THE EQUATION
C                    - AX=B, WHERE A IS M X NA WITH M GREATER THAN
C                    - OR EQUAL TO NA. INPUT A IS REPLACED BY
C                    - THE PSEUDO-INVERSE OF A
C                    B  - MATRIX OF THE RIGHT HAND SIDE OF THE EQUATION
C                    - AX=B, WHERE B IS M X NB. THE NA X NB
C                    - SOLUTION X OVERWRITES B.
C                    M  - NUMBER OF ROWS IN A AND B.
C                    NA - NUMBER OF COLUMNS IN MATRIX A
C                    NB - NUMBER OF COLUMNS IN MATRIX B
C                    IA - ROW DIMENSION OF A IN THE CALLING
C                    - PROGRAM.
C                    IB - ROW DIMENSION OF B IN THE CALLING
C                    - PROGRAM.
C                    IDGT - THE ELEMENTS OF A ARE ASSUMED TO BE CORRECT
C                    - TO IDGT SIGNIFICANT DIGITS. IDGT IS AN
C                    - INPUT PARAMETER.
C                    WKAREA - WORK AREA OF DIMENSION GREATER THAN OR EQUAL
C                    - TO NA(NA+4).
C                    IER - ERROR PARAMETER
C                    - TERMINAL ERROR = 12M + N
C                    - N = 1 INDICATES THAT INPUT A IS A ZERO
C                    - MATRIX.
C  PRECISION        - SINGLE
C  REQD. IMSL ROUTINES - LPSDOR,LSVALR,UEPTST,VSORTM
C  LANGUAGE          - FORTRAN
C-----

```

CALL LLSQAR (A,B,M,NA,NB,IA,IB,IDGT,WKAREA,IER)

Purpose

LLSQAR performs the least squares solution of an overdetermined system of linear equations. Given the M by NA matrix A and the M by NB matrix B, where M is not less than NA, this routine finds the NA by NB matrix X such that $\|X\|_E$ and $\|AX-B\|_E$ = minimum, where $\|\cdot\|_E$ is the Euclidean norm of a matrix. That is,

$$\|AX-B\|_E = \left[\sum_{i=1}^M \sum_{j=1}^{NB} \left(\sum_{k=1}^{NA} A_{ik} X_{kj} - B_{ij} \right)^2 \right]^{1/2}$$

Algorithm

The routine first calculates the pseudo-inverse of the matrix A, calling IMSL routine LPSDOR. $A^+ \equiv V(S^+)^T$. (See the documentation of LPSDOR.) V is an NA by NA orthogonal matrix, S^+ is an NA by NA diagonal matrix and U^T is an NA by M matrix with orthogonal rows. The solution of the equations is computed by $V(S^+)^T U^T B$.

Programming Notes

1. In the calling program, both A and B are two-dimensional arrays. The value of the first dimension of A is IA (IA not less than M), and the value of the first dimension of B is IB (IB not less than M).
2. The work area, WKAREA, must be a one-dimensional array of length at least NA(NA+4).
3. The input matrix A is replaced by the pseudo-inverse of A.
4. The NA by NB solution X overwrites input matrix B.

Accuracy

The elements of A are assumed to be correct to IDGT significant digits. The routine computes the pseudo-inverse of $\bar{A} = USV^T$; \bar{A} differs from A in the Euclidean norm by less than $d = \frac{M}{NA} * (\max_{i,j} a_{i,j}) * 10^{-IDGT}$, and of all matrices which differ from A by less than d in the Euclidean norm, \bar{A} has minimal rank.

Example

DIMENSION A(6,3), B(7,4), WKAREA(60)

Input:

M = 6
NA = 3
NB = 4
IA = 6
IB = 7
IDGT = 4

A = $\begin{bmatrix} 33.0 & 16.0 & 72.0 \\ -24.0 & -10.0 & -57.0 \\ -8.0 & -4.0 & -17.0 \\ 33.0 & 16.0 & 72.0 \\ -24.0 & -10.0 & -57.0 \\ -8.0 & -4.0 & -17.0 \end{bmatrix}$

B = $\begin{bmatrix} 1.0 & 0.0 & 0.0 & -359.0 \\ 0.0 & 1.0 & 0.0 & 281.0 \\ 0.0 & 0.0 & 1.0 & 85.0 \\ 1.0 & 0.0 & 0.0 & -359.0 \\ 0.0 & 1.0 & 0.0 & 281.0 \\ 0.0 & 0.0 & 1.0 & 85.0 \\ x & x & x & x \end{bmatrix}$

CALL LLSQAR (A,B,M,NA,NB,IA,IB,IDGT,WKAREA,IER)

Output:

X = $\begin{bmatrix} -9.6667 & -2.6667 & -32.000 & 1.0000 \\ 8.0000 & 2.5000 & 25.500 & -2.0000 \\ 2.6667 & .66667 & 9.0000 & -5.0000 \end{bmatrix}$

Note: x denotes an element which is not used by LLSQAR.

SUBROUTINE LPSDOR (A,M,N,IA,AINV,IDGT,WKAREA,IER)			LPSD0010
C			LPSD0020
C	C-LPSDOR-----S-----LIBRARY 3-----		LPSD0030
C			LPSD0040
C	FUNCTION	- PSEUDO-INVERSE OF A MATRIX.	LPSD0050
C	USAGE	- CALL LPSDOR (A,M,N,IA,AINV,IDGT,WKAREA,IER)	LPSD0060
C	PARAMETERS	A - A GIVEN MATRIX OF SIZE M X N	LPSD0070
C		M - NUMBER OF ROWS IN MATRIX A	LPSD0080
C		N - NUMBER OF COLUMNS IN MATRIX A	LPSD0090
C		IA - ROW DIMENSION OF A AND AINV IN CALLING	LPSD0100
C		PROGRAM (IA MUST BE GREATER THAN OR EQUAL	LPSD0110
C		TO M).	LPSD0120
C		AINV - THE TRANSPOSE OF THE PSEUDO-INVERSE OF A	LPSD0130
C		IS STORED IN THE M X N MATRIX AINV.	LPSD0140
C		IDGT - THE ELEMENTS OF A ARE ASSUMED TO BE CORRECT	LPSD0150
C		TO IDGT DECIMAL PLACES. IDGT IS AN INPUT	LPSD0160
C		PARAMETER.	LPSD0170
C		WKAREA - WORK AREA OF DIMENSION AT LEAST EQUAL TO	LPSD0180
C		N(N+4).	LPSD0190
C		IER - ERROR PARAMETER	LPSD0200
C		TERMINAL ERROR = 128 * N	LPSD0210
C		N = 1 INDICATES THAT A IS THE ZERO MATRIX	LPSD0220
C		TO IDGT ACCURACY (IN NORM).	LPSD0230
C	PRECISION	- SINGLE	LPSD0240
C	REQD. IMSL ROUTINES	- VSORTM,LSVALR,UENTST	LPSD0250
C	LANGUAGE	- FORTRAN	LPSD0260
C	-----		LPSD0270

CALL LPSDOR (A,M,N,IA,AINV,IDGT,WKAREA,IER)

Purpose

LPSDOR calculates the pseudo-inverse of the M by N matrix A with M not less than N.

Algorithm

The routine calculates the singular value decomposition of A by calling IMSL routine LSVALR.

$A = USV^T$, where U is an M by N matrix with orthonormalized columns, S is an N by N diagonal matrix containing the singular values of A, and V is an N by N orthogonal matrix. The pseudo-inverse is given by $V(S^{-1})U^T$.

Programming Notes

1. In the main program, both A and AINV are assumed to be of dimension M by N (IA not less than M). Thus the transpose of the pseudo-inverse of A is stored in AINV. AINV may occupy the same storage as does A, or completely separate storage.
2. The work area, WKAREA, must be a vector of length at least $N(N+4)$.
3. If A is the zero matrix, a terminal error message is printed, and the zero pseudo-inverse is not stored in AINV. Instead it will contain U.

Accuracy

The elements of A are assumed correct to IDGT significant digits. The routine computes the exact pseudo-inverse, without any roundoff error, to a matrix \bar{A} which differs by A in the Euclidean norm by less than 10^{-IDGT} , and which has minimal rank.

Identification:

INTERP Aitken's Kth Degree Polynomial Interpolation of Tabular Data
CDC 6600 FORTRAN Subroutine Subprogram

Purpose:

Given an ascending or descending table X(I) of independent variables and a corresponding table Y(I) of dependent variables, subroutine INTERP computes a Kth degree polynomial interpolated value YO for a given abscissa XO. If the argument falls outside the range of tabular values, extrapolation is performed.

Control:

```
DIMENSION X(N), Y(N), TEMP(2*(K+1))  
CALL INTERP (X,Y,N,K,XO,YO,TEMP,IER)
```

where:

X(I) List of values of the independent variable in either ascending or descending order
Y(I) List of the corresponding values of the dependent variable
N Number of X, Y pairs
K Degree of the interpolating polynomial (K less than N)
XO Point at which interpolation is requested
YO The computed interpolated value
TEMP A one-dimensional array of 2*(K+1) words of temporary storage
IER = 0 Interpolation successfully performed
= 1 Extrapolation successfully performed
= 2 Either degree of interpolation out of range or two identical independent variables.

Method:

Repeated bisection of the index (subscript) of the list of values of X is carried out until the argument is isolated between two consecutive values. Then Aitken's recursion of linear interpolation is performed using an equal number of points on either side of XO and, for even degrees, one additional point nearest XO.

Remarks:

The user is cautioned that increasing the degree of the fitted polynomial does not necessarily increase the "accuracy" of the interpolation. Indeed, this may introduce spurious oscillations into the interpolated values since the higher the degree of a polynomial, the more relative maxima and minima it can have. In particular, if the tabular data involves appreciable "noise", then use of a technique which "smooths" rather than one which "fits" (as does INTERP) may be more appropriate.

The user is also encouraged to test to see if IER = 2 if there is any question concerning the uniqueness of the independent variables.

Storage:

INTERP uses 2548 words of storage and no common.

References:

F. B. Hildebrand, Introduction to Numerical Analysis, McGraw-Hill, New York/Toronto/London, 1956, pp. 49-50.

REFERENCES

1. Waters, J.P., Aas, H.G., and Erf, R.K., "Investigation of Applying Interferometric Holography to Turbine Blade Stress Analysis", UARL Final Report J9907PA-13 (Naval Air Systems Command Contract N00019-69-C-0271), Feb 1970.
2. Taylor, L.H., and Brandt, G.B., "An Error Analysis of Holographic Strains Determined by Cubic Splines", Experimental Mechanics, Vol. 12, No. 12, pp 543-548, Dec 1972.
3. Danliker, R., Eliasson, B., Ineichen, B., Mastner, F.M., "Quantitative Determination of Bending and Torsion Through Holographic Interferometry", Brown Boveri Research Report KLR-74-21, Baden, Switzerland, Dec 1974.
4. Rayleigh, J.W.S., The Theory of Sound, Vol. 1, Dover Publications, Inc., New York, 1945.
5. Szilard, R., Theory and Analysis of Plates, Prentice-Hall, Inc., Englewood Cliffs, New Jersey, 1974.
6. Young, D., "Vibration of Rectangular Plates by the Ritz Method", J. Applied Mechanics, Vol. 17, No. 4, Dec 1950, pp 448-453.
7. Powell, R.L., and Stetson, K.A., "Interferometric Vibration Analysis by Wavefront Reconstruction", J. Optical Society America, Vol. 55, Dec 1965, p. 1593.
8. Brown, G.M., Grant, R.M., Stroke, G.W., "Theory of Holographic Interferometry", J. Acoustical Society of America, Vol. 45, No. 5, 1969, pp 1166-1179.
9. Moore, E.H., "Memoirs of the American Philosophical Society (General Analysis, Part I)", Vol. 1, 1935.
10. Penrose, R., "A Generalized Inverse for Matrices", Proc. Cambridge Philosophical Society, Vol. 51, 1955, pp 406-413.
11. Golub, G.H., and Reinsch, C., "Singular Value Decomposition of Least Squares Solutions", Numer. Math., Vol. 14, 1970, pp 403-420.
12. Greville, T.N.E., "The Pseudoinverse of a Rectangular or Singular Matrix and its Application to the Solution of Systems of Linear Equations", SIAM Review, Vol. 1, No. 1, Jan 1959, pp 38-43.